Bioorganic Chemistry xxx (xxxx) xxx

Contents lists available at ScienceDirect

Bioorganic Chemistry

journal homepage: www.elsevier.com/locate/bioorg

Synthesis, biological evaluation and QSAR studies of new thieno[2,3-*d*]pyrimidin-4(3*H*)-one derivatives as antimicrobial and antifungal agents

George E. Magoulas [a,1], Lefkothea Kalopetridou [a,1], Ana Ćirić [b], Eftichia Kritsi [a], Paraskevi Kouka [a], Panagiotis Zoumpoulakis [a], Niki Chondrogianni [a], Marina Soković [b], Kyriakos C. Prousis [a], Theodora Calogeropoulou [a,*]

[a] National Hellenic Research Foundation, Institute of Chemical Biology, 48 Vassileos Constantinou Avenue, 11653 Athens, Greece
[b] University of Belgrade, Institute for Biological Research "Siniša Stanković" – National Institute of Republic of Serbia, Blvd. despot Stefan 142, 11000 Belgrade, Serbia

ARTICLE INFO

Keywords:
Thienopyrimidinones
Antimicrobial activity
Toxicity studies
Pharma RQSAR

ABSTRACT

A series of new thieno[2,3-*d*]pyrimidin-4(3*H*)-one derivatives were synthesized and evaluated for their activity against four gram-positive and four gram-negative bacterial and eight fungal species. The majority of the compounds exhibited excellent antimicrobial and antifungal activity, being more potent than the control compounds. Compound **22**, bearing a *m*-methoxyphenyl group and an ethylenediamine side chain anchored at C-2 of the thienopyrimidinone core, is the most potent antibacterial compound with broad antimicrobial activity with MIC values in the range of 0.05–0.13 mM, being 6 to 15 fold more potent than the controls, streptomycin and ampicillin. Furthermore, compounds **14** and **15** which bear a *p*-chlorophenyl and *m*-methoxyphenyl group, respectively, and share a 2-(2-mercaptoethoxy)ethan-1-ol side chain showed the best antifungal activity, being 10–15 times more potent than ketoconazole or bifonazole with MIC values 0.013–0.026 and 0.027 mM, respectively. Especially in the case of compound **15** the low MIC values were accompanied by excellent MFC values ranging from 0.056 to 0.058 mM. Evaluation of toxicity *in vitro* on HFL-1 human embryonic primary cells and *in vivo* in the nematode *C. elegans* revealed no toxic effects for both compounds **15** and **22** tested at the MIC concentrations. Ligand-based similarity search and molecular docking predicted that the antibacterial activity of analogue **22** is related to inhibition of the topoisomerase II DNA gyrase enzyme and the antifungal activity of compound **15** to CYP51 lanosterol demethylase enzyme. R-Group analysis as a means of computational structure activity relationship tool, highlighted the compounds' crucial pharmacophore features and their impact on the antibacterial and antifungal activity. The presence of a *N*-methyl piperidine ring fused to the thienopyrimidinone core plays an important role in both activities.

1. Introduction

Infectious diseases caused by bacteria and fungi emerged and still evolve side by side with life itself. They have played a very important role in the history of mankind, even changing the course of events in terms of war, migration of population etc. From the empirical use of plant extracts during ancient times to the impressive advance of modern medicine, the ceaseless effort of humans to subdue infectious diseases is evident. However, this is battle has not been completely won yet. The abundance of new and effective antimicrobial drugs comes along with their misuse or overuse leading eventually to antimicrobial resistance (AMR). According to WHO, AMR is considered the cause of at least 700,000 deaths annually, mainly in developing countries, with considerable economic consequences [1]. Thus, there is still an unmet need for new antimicrobial drugs with reduced toxicity and activity against resistant strains.

Heterocycles and especially fused heterocyclic rings play a significant role in medicinal chemistry as they can be found in many approved drugs, exhibiting a wide range of biological activities [2,3].

Thienopyrimidinones represent a scaffold that has drawn much attention as a source of bioactive compounds. A large number of derivatives containing the thienopyrimidinone moiety were evaluated as MCH-R1 [4] and mGluR1 antagonists [5], or as FGFR1 kinase [6], PARP-1 [7], SIRT-2 [8] and phosphodiesterase 7 inhibitors [9]. Additionally,

* Corresponding author at: Institute of Chemical Biology, National Hellenic Research Foundation, 48 Vassileos Constantinou Avenue, 11635 Athens, Greece.
E-mail address: tcalog@eie.gr (T. Calogeropoulou).
[1] Equally contributed.

https://doi.org/10.1016/j.bioorg.2020.104509
Received 12 September 2020; Received in revised form 11 November 2020; Accepted 19 November 2020
Available online 26 November 2020

this class of compounds has shown anti-malarial [10], anti-tubercular [11], antiviral [12], anti-inflammatory and antimicrobial properties [13,14].

Inspired by the broad-spectrum activity of the thienopyrimidinone compound class, we embarked upon the synthesis of twelve new derivatives bearing structural modifications for SAR purposes concerning their antibacterial and antifungal properties. More specifically: (a) a phenyl ring substituted by electron-donating (-OMe) or electron-withdrawing (-Cl) group, was introduced at the *N*-3 position of the thieno[2,3-*d*]pyrimidin-4(3*H*)-one skeleton; (b) biocompatible aliphatic amines or an ethoxyethanol group were anchored at the C-2 position through a sulfur bridge or an amino group for enhanced hydrophilicity and (c) a *N*-methylpiperidine or a cyclohexane moiety was fused to the core. The changes that were applied to the thieno[2,3-*d*]pyrimidin-4(3*H*)-one core are summarized in Fig. 1.

All new compounds (**14**–**16**, **18**–**20**, **22**–**25** and **31**–**33**) were evaluated *in vitro* for their antimicrobial and antifungal activity against eight Gram-negative and Gram-positive bacterial species and eight fungi, respectively.

2. Results and discussion

2.1. Chemistry

The synthetic strategy followed for the preparation of compounds **14**–**16** is depicted in Scheme 1. A Gewald reaction between the commercially available *N*-methyl pyrrolidone **1** and ethyl cyanoacetate **2**, in the presence of sulfur and diethylamine in MeOH under microwave irradiation, afforded the 2-aminothiophene derivative **3** in 69% yield [15]. The latter reacted with the corresponding substituted aryl-isothiocyanates **4**–**6** in a SN_2 fashion in the presence of pyridine. The reaction proceeded either by conventional heating or by using microwave irradiation to give thioureas **7**–**9** in 45–80% yield. The final compounds **14**–**16** were obtained, in 60–72% yield, in a one-pot reaction which initially involved the cyclization of thioureas **7**–**9** to the corresponding potassium thiolate salts **10**–**12**, upon treatment with ethanolic KOH solution under reflux, followed by the addition of monotosylated diethylene glycol **13**.

The synthesis of compounds **18**–**20** was accomplished in an analogous manner as described above. Thus, treatment of thiourea derivative **7** with ethanolic KOH afforded the intermediate thiolate **10** which was converted to the *S*-methylated compound **17**, in 97% yield, upon addition of iodomethane. Subsequently, compound **17** was reacted under solvent-free conditions with a large excess of propane-1,3-diamine or butane-1,4-diamine or 3-aminopropan-1-ol to afford the desired compounds **18**–**20**, respectively in 46–55% yield (Scheme 2).

Compounds **22** and **24**, **25** were obtained following the same methodology as above for compound **17**, using the previously synthesized thiourea derivative **8** to obtain the *S*-methylated compound **21**. Reaction of **21** under solvent-free conditions with a large excess of ethane-1,2-diamine, propane-1,3-diamine, or 2-(piperazin-1-yl)ethane-1-amine at elevated temperatures above 100 °C, gave compounds **22** and **24**, **25**, respectively, although in very low yields 10–28%. In the case of ethane-1,2-diamine, compound **23** [16] was also obtained in 39% yield along with compound **22** (see Scheme 3).

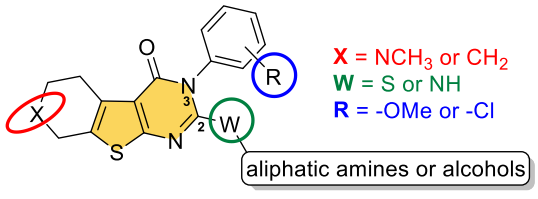

Fig. 1. General structure of the new thieno[2,3-*d*]pyrimidin-4(3*H*)-one derivatives (**14**–**16**, **18**–**20**, **22**–**25** and **31**–**33**).

Finally, the synthesis of the targeted compounds **31**–**33** was realized using the synthetic methodology followed above for thioureas **7**–**9**, starting from the commercially available cyclohexanone (**26**) (Scheme 4). Condensation of **26** with ethyl cyanoacetate (**2**) led to 2-aminothiophene **27** in 52% yield. The latter was reacted with 3-methoxy benzene isothiocyanate (**5**) to give thiourea **28** [17] in 95% yield which, in turn, was converted to thiolate **29** in the presence of ethanolic KOH solution and finally to the *S*-methylated compound **30** upon treatment with iodomethane. Reaction of compound **30** with ethane-1,2-diamine, or propane-1,3-diamine or 2-(piperazin-1-yl)ethane-1-amine under solvent-free conditions at elevated temperatures, afforded compounds **31**–**33**, respectively in 20–74% yield.

2.2. Antimicrobial evaluation

2.2.1. Evaluation of in vitro antibacterial activity

The antibacterial activity of all synthesized compounds (including side-product **23**) was evaluated against four gram-positive (*Bacillus. cereus, Micrococcus flavus, Staphylococcus aureus,* and *Listeria monocytogenes*) and four gram-negative (*Escherichia coli, Enterobacter cloacae, Pseudomonas aeruginosa,* and *Salmonella typhimurium*) bacterial strains, using streptomycin and ampicillin as controls. The results are displayed in Table 1 as minimal inhibitory concentrations (MICs), the lowest concentration that inhibits the growth of the bacteria, and minimal bactericidal concentrations (MBCs), the lowest concentration that kills 99.5% of the bacteria.

In detail, compounds **14** and **16** bearing a 2(2-thio)ethoxy)ethanol side chain and a 4-chlorophenyl or 4-methoxyphenyl substituent at *N*-3, respectively, showed very good antimicrobial activity. In particular, analogue **16** was very potent against gram-negative bacteria, exhibiting higher activity than streptomycin or ampicillin with MIC values ranging between 0.02 and 0.22 mM while the MCB was 0.45 ± 0.00 mM. In addition, compound **16** was also more potent than the controls against the gram positive bacteria *B. cereus* and *M. flavus* exhibiting MIC and MBC values of 0.11 ± 0.01 mM and 0.45 ± 0.05 mM, respectively. Replacement of the C-2 2(2-thio)ethoxy)ethanol side chain in compound **14** by ω-diamines or a 3-hydroxypropylamine (compounds **18**–**20**) resulted in a slight decrease in the activity. However, the 4-hydroxybutylamine-substituted compound **19** was more potent than **14** against *M. flavus* and *P. aeruginosa* with MIC = 0.06 ± 0.005 mM and MCB = 0.45 ± 0.00 mM. The C-2 amino-substituted congeners of compound **15**, derivatives **22, 24** and **25**, possess good to excellent activities against all bacterial strains tested. The most potent was compound **22** bearing an ethylene diamine side chain, which exhibited an impressive broad-spectrum antimicrobial activity with MIC (MBC) values ranging between 0.05 (0.06) and 0.13(0.26) mM, thus, being 6–15 fold more potent than the controls, streptomycin and ampicillin. The elongation of the C-2 side chain by one carbon in compound **24** reduces significantly the antimicrobial activity which is even more pronounced in **25** which bears a constrained piperazinyl-substituted side chain. Compound **23**, which was isolated as a side product towards the synthesis of **22**, possessed low activity, suggesting the importance of an aryl substitution at the *N*-3 position of the thieno[2,3-*d*]pyrimidin-4(3*H*)-one core.

Since the 3-methoxyphenyl substituted series resulted in the most potent derivative **22** we set out to explore the effect of the *N*-methyl piperidine moiety on the antimicrobial activity, by the synthesis of the cyclohexyl-substituted derivatives **31**–**33**. As a first observation all the new compounds **31**–**33** were less potent than their *N*-methyl piperidine congeners **22, 24** and **25**. The most potent was the C-2 (2-aminoethyl-amine)-substituted derivative **31**, being more active than streptomycin or ampicillin in almost all the bacterial strains tested, with MIC values ranging between 0.18 and 0.36 mM and MBC values ranging between 0.36 and 0.73 mM. However, compound **31** was less potent than its *N*-methyl piperidine congener **22.**

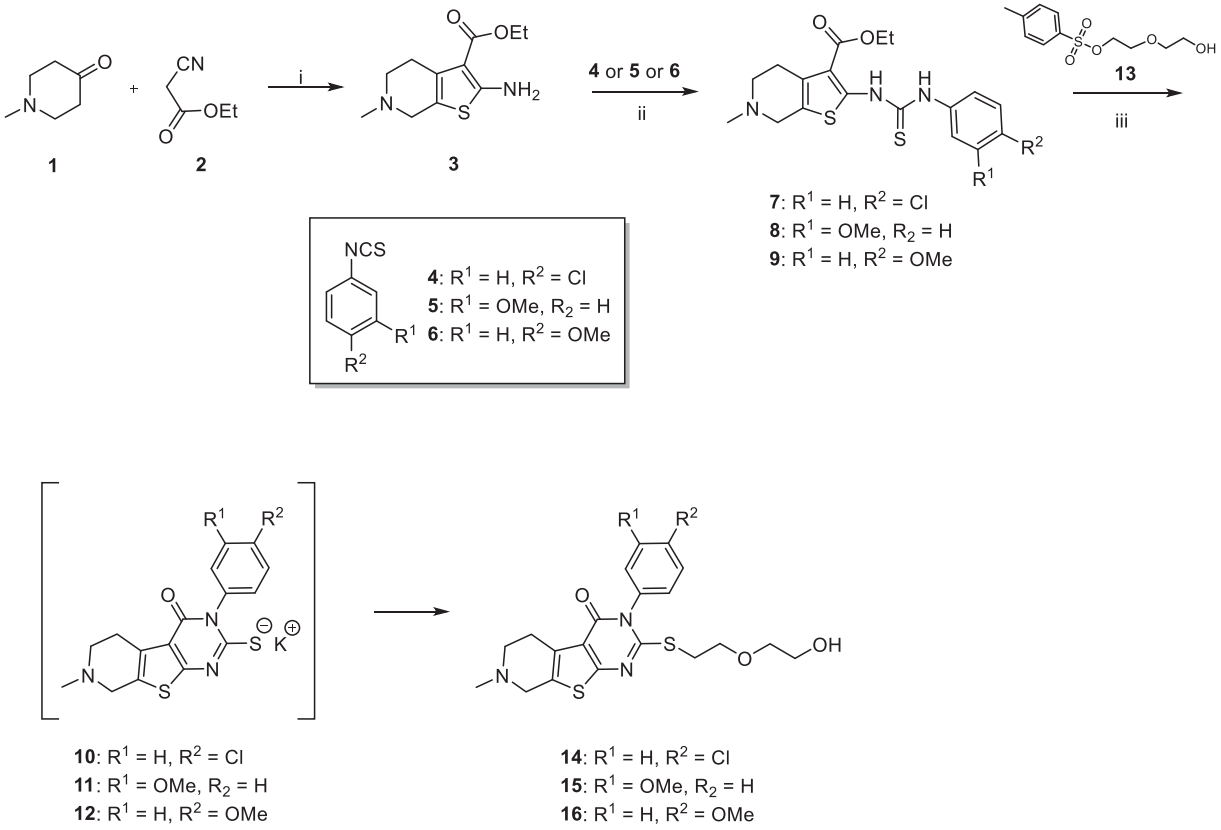

Scheme 1. Synthesis of compounds **14**–**16**. *Reagents and conditions:* (i) Sulfur, diethylamine, MeOH, μW, T = 100 °C, t = 4 min, P = 120 W; (ii) Method A: pyridine, 45 °C, 16 h or method B: pyridine, μW, T = 100 °C, t = 2 min, P = 150 W; (iii) (a) Ethanolic KOH, reflux; (b) EtOH, reflux, 18 h.

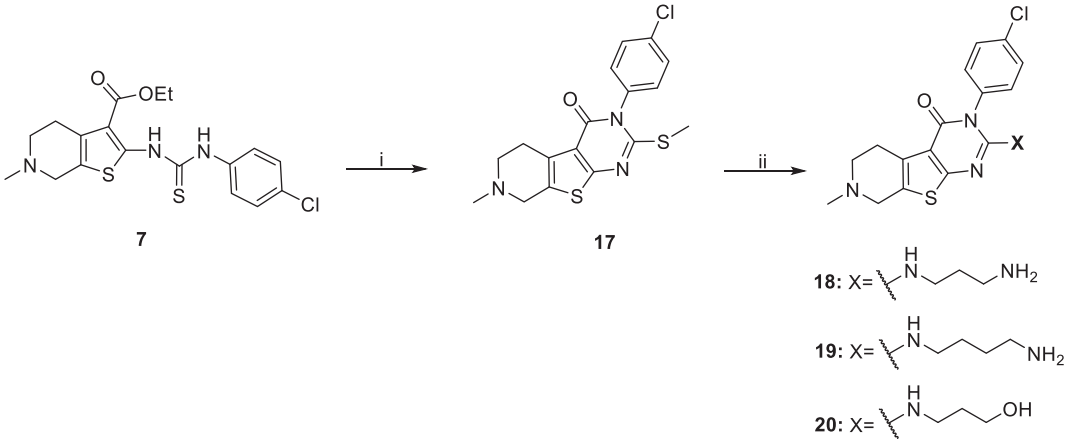

Scheme 2. Synthesis of compounds **18**–**20**. *Reagents and conditions:*(i) (a) Ethanolic KOH, reflux; (b) Iodomethane, ethanol, rt. 1 h; (ii) Propane-1,3-diamine (30 eq), 100 °C, 16 h, or butane-1,4-diamine (30 eq) 140 °C, 16 h, or 3-aminopropan-1-ol, (30 eq), 150 °C, 16 h.

2.2.2. Evaluation of in vitro antifungal activity

All the new compounds were also tested for their antifungal activity against eight fungal species namely, *Aspergillus fumigatus, Aspergillus versicolor, Aspergillus ochraceus, Aspergillus niger, Trichoderma viride, Penicillium funiculosum, Penicillium ochrochloron,* and *Penicillium verrucosum* var. *cyclopium.* Ketoconazole and bifonazole were used as controls. The antifungal activity is presented in Table 2, as the minimal minimal inhibitory concentration (MIC) and the minimal fungicidal concentration (MFC).

The most potent compound among derivatives **14**–**16** which bear a 2 (2-thio)ethoxy)ethanol group at C-2, is the *N*-3-(3-methoxyphenyl)-substituted compound **15**. It exhibits 10–100 fold higher activity than ketoconazole and 17–23 fold higher activity than bifonazole. Interestingly, compound **15** not only presents high potency against all the fungi tested but in addition a very low MFC value of 0.056 ± 0.005 mM. Compounds **14** and **16** were also more potent than the controls with MIC values ranging from 0.013 to 0.027 mM, but the MFC values were higher than those of **15**. Replacement of the C-2 side chain of compound **14** with ω-diamines (compounds **18** and **19**) resulted in a slight improvement in activity for the 3-aminopropylamino C-2-substituted derivative **18** (MIC (MFC) values 0.015 (0.233) mM). Furthermore, the 4-aminobutylamino C-2-substituted derivative **19** possessed similar activity to **14** with MIC values ranging between 0.029 and 0.255 mM and MFC between 0.06 and 0.112 mM. Conversely, the C-2 substituted 3-

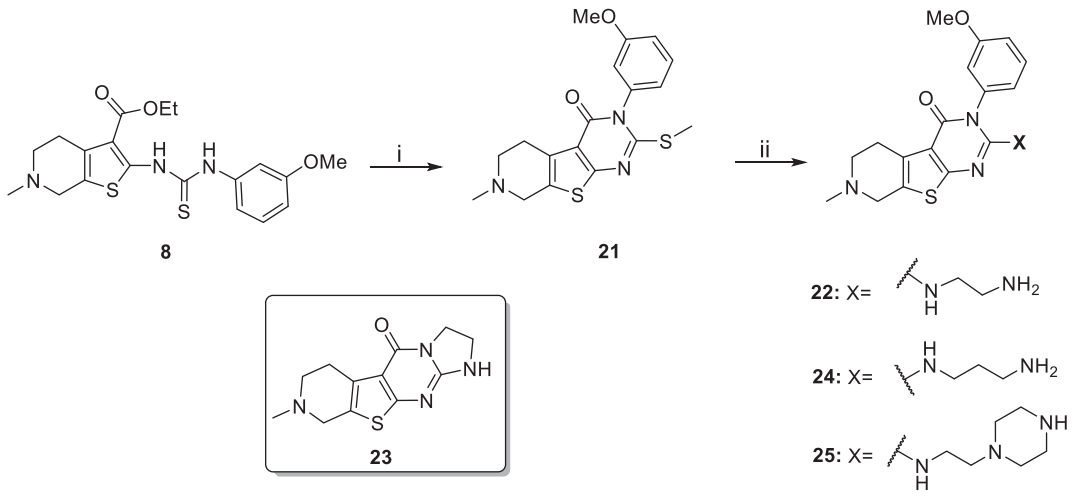

Scheme 3. Synthesis of compounds **22**, **24** and **25**. *Reagents and conditions:*(i) (a) Ethanolic KOH, reflux; (b) Iodomethane, ethanol, rt, 1 h; (ii) Ethane-1,2-diamine (35 eq), 100 °C, 72 h, or propane-1,3-diamine (30 eq), 120 °C, 72 h, or 2-(piperazin-1-yl)ethane-1-amine (56 eq), 130 °C, 72 h.

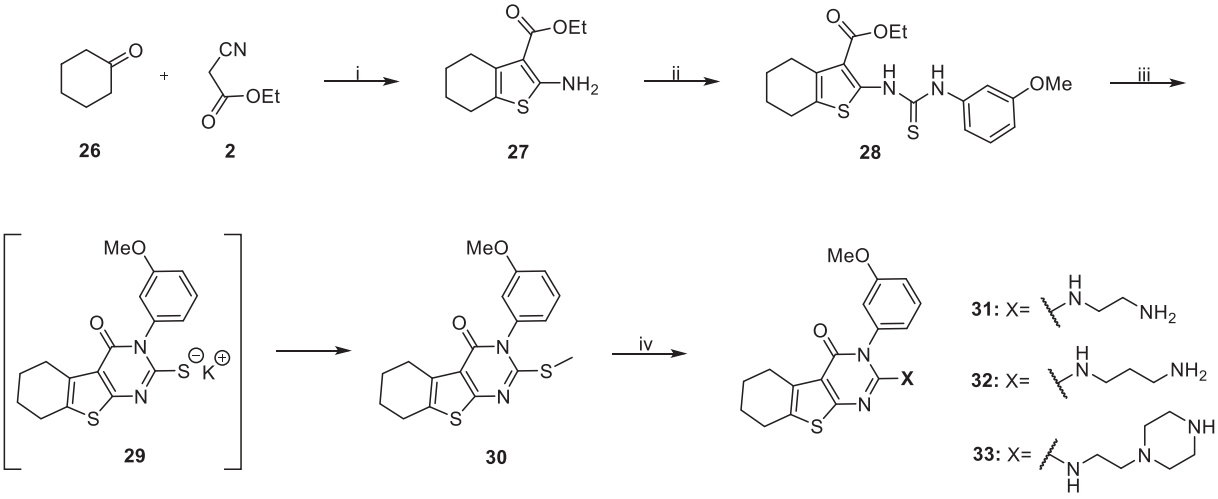

Scheme 4. Synthesis of compounds **31**–**33**. *Reagents and conditions:* (i) Sulfur, diethylamine, MeOH, μW, T = 100 °C, t = 2 min, P = 150 W; (ii) **5**, pyridine, 45 °C, 18 h; (iii) (a) Ethanolic KOH, reflux; (b) Iodomethane, ethanol, rt. 1 h; (iv) Ethane-1,2-diamine (69 eq), 100 °C, 48 h or propane-1,3-diamine (47 eq) 140 °C, 18 h, or 2-(piperazin-1-yl)ethane-1-amine (52 eq), 140 °C, 18 h.

aminopropanol derivative **20** presented moderate activity against the majority of the fungal strains tested. The C-2 amino-substituted congeners of compound **15**, derivatives **22, 24** and **25** presented slightly reduced antifungal activity with respect to the parent compound. However, derivative **22** was more potent than the controls against the eight fungal strains tested. Surprisingly, compound **23**, which lacks both the *N*-3-aryl group and the C-2 side chain, showed significant inhibitory and fungicidal potency with MIC value 0.046 ± 0.01 mM (0.041 ± 0.01 for *A. niger*) and MFC value 0.095 ± 0.03 mM against all the tested fungi.

Finally, the replacement of the *N*-methyl piperidine moiety by a cyclohexane ring (compounds **31**–**33**) led to significant loss of activity.

2.3. Evaluation of in vitro and in vivo toxicity

As discussed above the most potent antibacterial agent was compound **22**, presenting broad spectrum activity with MIC (MBC) values ranging between 0.05 (0.06) and 0.06 (0.26) mM against all strains tested. In addition, the most potent antifungal agent was compound **15** with MIC = 0.027 ± 0.005 mM and MFC = 0.056 ± 0.005 mM against all fungal strains tested. To obtain a better understanding as to whether the antimicrobial effect of these compounds was specific and not due to general toxicity, compounds **15** and **22** were further investigated for their potential toxic effects *in vitro* on HFL-1 human embryonic primary cells and *in vivo* in an established model for toxicity testing [18,19], namely the nematode *C. elegans*. Both cells and nematodes were exposed to the concentrations corresponding to the (MIC) /MFC values for compound **15** and the MIC (0.05 mM) /highest MBC (0.26 mM) values for compound **22**.

Toxicity testing in human primary fibroblasts is more appropriate as compared to cancer or immortalized cells since primary cells are the ones that will be most probably affected by a potential antimicrobial or antifungal treatment. Thus, concerning the *in vitro* toxicity, the number of living cells was determined through crystal violet staining after 24 and 48 h of exposure to each compound, while DMSO was added in control cultures. Both compounds were not toxic at the concentrations tested since they did not induce any significant changes in the survival of HFL-1 human primary fibroblasts (Fig. 2).

Subsequently, the toxicity of compounds **15** and **22** was evaluated on the multicellular organism *C. elegans*. Standardized toxicity tests using this nematode have been introduced since 1990s [20] to define a variety of endpoints for toxic effects [21,22]. Screening of drug and pollutants toxicity has been shown to induce marked effects on various phenotypic

Table 1
In vitro antibacterial activity of compounds **14**–**16**, **18**–**20**, **22**–**25** and **31**–**33**.

Compounds	MIC/MBC (mM)								
		B.c.	*M.f.*	*S.a.*	*L.m.*	*E.c.*	*En. cl.*	*P.a.*	*S.t.*
14	**MIC**	0.11 ± 0.01^{b}	0.44 ± 0.08^{d}	0.11 ± 0.01^{b}	0.44 ± 0.01^{b}	0.44 ± 0.01^{c}	0.22 ± 0.02^{b}	0.22 ± 0.02^{b}	0.22 ± 0.02^{b}
	MBC	0.22 ± 0.02^{b}	0.88 ± 0.05^{bc}	0.22 ± 0.02^{b}	1.77 ± 0.30^{c}	0.88 ± 0.05^{b}	0.44 ± 0.02^{b}	0.44 ± 0.02^{b}	0.44 ± 0.02^{b}
15	**MIC**	0.56 ± 0.05^{d}	2.23 ± 0.25^{f}	0.56 ± 0.05^{d}	4.47 ± 0.28^{e}	2.23 ± 0.25^{e}	2.23 ± 0.25^{d}	2.23 ± 0.25^{d}	2.23 ± 0.25^{e}
	MBC	4.47 ± 1.12^{ef}	4.47 ± 0.28^{ef}	4.47 ± 0.28^{de}	8.94 ± 1.23^{f}	4.47 ± 0.28^{d}	4.47 ± 0.28^{de}	4.47 ± 0.28^{e}	4.47 ± 0.28^{e}
16	**MIC**	0.11 ± 0.01^{b}	0.11 ± 0.03^{b}	0.22 ± 0.02^{c}	0.45 ± 0.00^{b}	0.04 ± 0.002^{a}	0.02 ± 0.01^{a}	0.04 ± 0.02^{a}	0.22 ± 0.02^{b}
	MBC	0.45 ± 0.05^{c}	0.45 ± 0.00^{ab}	0.45 ± 0.00^{bc}	0.89 ± 0.06^{b}	0.45 ± 0.00^{ab}	0.45 ± 0.00^{b}	0.45 ± 0.00^{b}	0.45 ± 0.00^{b}
18	**MIC**	0.12 ± 0.04^{b}	0.50 ± 0.00^{d}	0.12 ± 0.04^{b}	0.50 ± 0.00^{b}	1.24 ± 0.10^{de}	0.25 ± 0.00^{b}	0.25 ± 0.00^{b}	0.25 ± 0.00^{b}
	MBC	0.25 ± 0.02^{b}	2.48 ± 0.30^{d}	0.25 ± 0.00^{b}	2.48 ± 0.30^{d}	2.48 ± 0.30^{c}	0.50 ± 0.00^{b}	0.50 ± 0.00^{b}	0.50 ± 0.00^{b}
19	**MIC**	0.11 ± 0.01^{b}	0.06 ± 0.005^{a}	0.24 ± 0.02^{c}	0.45 ± 0.00^{b}	0.22 ± 0.02^{b}	0.45 ± 0.00^{c}	0.06 ± 0.005^{a}	0.22 ± 0.02^{b}
	MBC	0.45 ± 0.05^{c}	0.45 ± 0.00^{b}	0.45 ± 0.00^{bc}	0.90 ± 0.03^{b}	0.45 ± 0.00^{ab}	0.90 ± 0.03^{c}	0.45 ± 0.00^{b}	0.45 ± 0.02^{b}
20	**MIC**	0.25 ± 0.05^{c}	0.25 ± 0.00^{c}	0.49 ± 0.03^{d}	0.49 ± 0.03^{b}	0.25 ± 0.00^{b}	0.49 ± 0.03^{c}	0.25 ± 0.00^{b}	0.49 ± 0.03^{c}
	MBC	0.49 ± 0.06^{c}	0.49 ± 0.03^{b}	0.99 ± 0.03^{c}	0.99 ± 0.03^{b}	0.49 ± 0.03^{ab}	0.99 ± 0.03^{c}	0.49 ± 0.03^{b}	0.99 ± 0.03^{c}
22	**MIC**	$\mathbf{0.05} \pm 0.001^{a}$	$\mathbf{0.13} \pm 0.01^{b}$	$\mathbf{0.05} \pm 0.005^{a}$	$\mathbf{0.06} \pm 0.005^{a}$	$\mathbf{0.06} \pm 0.005^{a}$	$\mathbf{0.05} \pm 0.001^{a}$	$\mathbf{0.05} \pm 0.001^{a}$	$\mathbf{0.05} \pm 0.001^{a}$
	MBC	$\mathbf{0.06} \pm 0.001^{a}$	$\mathbf{0.26} \pm 0.02^{a}$	$\mathbf{0.06} \pm 0.003^{a}$	$\mathbf{0.26} \pm 0.03^{a}$	$\mathbf{0.13} \pm 0.01^{a}$	$\mathbf{0.06} \pm 0.003^{a}$	$\mathbf{0.06} \pm 0.003^{a}$	$\mathbf{0.06} \pm 0.003^{a}$
23	**MIC**	2.67 ± 1.12^{f}	2.67 ± 0.16^{f}	0.76 ± 0.33^{de}	5.72 ± 1.18^{f}	2.67 ± 0.16^{e}	0.76 ± 0.33^{c}	0.76 ± 0.33^{c}	1.52 ± 0.16^{d}
	MBC	5.72 ± 1.18^{f}	5.72 ± 0.33^{f}	5.72 ± 0.33^{e}	11.44 ± 2.2^{g}	5.72 ± 0.33^{e}	5.72 ± 0.33^{e}	5.72 ± 0.33^{f}	5.72 ± 0.33^{e}
24	**MIC**	0.25 ± 0.05^{c}	0.13 ± 0.03^{b}	0.50 ± 0.15^{d}	1.00 ± 0.00^{c}	0.06 ± 0.005^{a}	0.50 ± 0.05^{c}	0.06 ± 0.005^{a}	0.50 ± 0.00^{c}
	MBC	1.00 ± 0.1^{d}	1.00 ± 0.00^{c}	1.00 ± 0.00^{c}	2.00 ± 0.15^{c}	0.50 ± 0.05^{ab}	1.00 ± 0.00^{c}	0.50 ± 0.05^{b}	1.00 ± 0.00^{c}
25	**MIC**	1.65 ± 0.9^{e}	2.20 ± 0.43^{f}	2.20 ± 0.43^{f}	4.40 ± 0.60^{e}	2.20 ± 0.43^{e}	2.20 ± 0.05^{b}	2.20 ± 0.05^{d}	4.40 ± 0.22^{f}
	MBC	3.30 ± 1.56^{e}	3.30 ± 0.06^{e}	4.40 ± 0.20^{de}	8.80 ± 1.15^{f}	4.40 ± 0.20^{d}	4.40 ± 0.05^{b}	4.40 ± 0.05^{e}	8.80 ± 0.60^{f}
31	**MIC**	0.18 ± 0.04^{bc}	0.18 ± 0.01^{bc}	0.18 ± 0.01^{bc}	0.36 ± 0.06^{b}	0.18 ± 0.01^{b}	0.18 ± 0.01^{b}	0.18 ± 0.01^{b}	0.18 ± 0.01^{b}
	MBC	0.36 ± 0.06^{bc}	0.36 ± 0.06^{a}	0.36 ± 0.06^{bc}	0.73 ± 0.15^{ab}	0.36 ± 0.06^{ab}	0.36 ± 0.06^{ab}	0.36 ± 0.05^{b}	0.36 ± 0.05^{b}
32	**MIC**	1.77 ± 0.9^{e}	1.77 ± 0.12^{e}	1.77 ± 0.12^{e}	3.54 ± 0.15^{c}	2.66 ± 0.16^{e}	1.77 ± 0.12^{d}	0.89 ± 0.09^{c}	1.77 ± 0.12^{d}
	MBC	3.54 ± 1.15^{e}	3.54 ± 0.67^{e}	3.54 ± 0.67^{d}	6.20 ± 0.15^{c}	3.54 ± 0.67^{cd}	3.54 ± 0.67^{d}	3.54 ± 0.67^{d}	3.54 ± 0.67^{d}
33	**MIC**	2.84 ± 0.9^{f}	2.27 ± 0.25^{f}	4.55 ± 0.30^{g}	4.55 ± 0.15^{d}	2.27 ± 0.25^{e}	4.55 ± 0.30^{e}	2.84 ± 0.30^{d}	2.84 ± 0.30^{e}
	MBC	$5.69 \pm 0.1.15^{f}$	2.84 ± 0.30^{d}	5.69 ± 1.15^{e}	5.69 ± 1.15^{e}	2.84 ± 0.90^{c}	5.69 ± 1.15^{e}	5.69 ± 1.15^{f}	5.69 ± 0.15^{e}
Streptomycin	**MIC**	0.18 ± 0.01^{bc}	0.35 ± 0.025^{cd}	0.09 ± 0.03^{ab}	0.35 ± 0.025^{b}	0.35 ± 0.025^{cd}	0.53 ± 0.05^{c}	0.35 ± 0.025^{bc}	0.35 ± 0.025^{bc}
	MBC	0.35 ± 0.01^{bc}	0.53 ± 0.05^{b}	0.18 ± 0.02^{b}	0.53 ± 0.05^{ab}	0.53 ± 0.05^{ab}	0.89 ± 0.09^{bc}	0.53 ± 0.05^{b}	0.53 ± 0.05^{b}
Ampicillin	**MIC**	0.86 ± 0.04^{d}	0.86 ± 0.04^{de}	0.86 ± 0.04^{de}	1.14 ± 0.15^{c}	0.86 ± 0.04^{d}	1.14 ± 0.15^{cd}	2.29 ± 0.25^{d}	0.86 ± 0.04^{cd}
	MBC	1.14 ± 0.15^{d}	1.14 ± 0.15^{c}	1.14 ± 0.15^{c}	2.29 ± 0.25^{c}	0.94 ± 0.03^{b}	1.51 ± 0.06^{c}	2.35 ± 0.10^{c}	0.94 ± 0.03^{c}

B.c.: B. cereus, M.f.: M. flavus, S.a.: S. aureus, L.m.: L. monocytogenes, E.c.: E. coli, En.cl.: En. cloacae, P.a.: P. aeruginosa, S.t.: S. typhimurium.
Values are expressed as means ± SD. Different letters in each column indicate statistically significant differences between samples ($p < 0.05$).

characteristics of *C. elegans* such as pharyngeal pumping rate, defecation rhythm, locomotion, development and reproduction [23–25]. Consequently, three phenotypic characteristics of the wild type (wt) animals were evaluated upon treatment with the tested compounds, namely the pharyngeal pumping rate, the defecation rate and the developmental timing which have been previously shown to respond to various toxic treatments [18,26]. Day 1 is considered as short-term exposure while day 3 as long-term exposure. Regarding the effects observed following exposure to compounds **15** and **22** at the MIC concentrations all phenotypic characteristics, including developmental timing, did not show any significant changes at any time point with the exception of a slight deceleration in the defecation rate at day 1 and a slight decrease in the pharyngeal pumping rate at day 3 of the animals treated with 0.05 mM compound **22** (Table 3). Therefore, based on this model, both compounds may be considered as non-toxic at MIC concentrations. With regard to exposure to compound **15** at the MFC concentration, a significant change was observed at day 1 for the pharyngeal pumping rate (but no difference during the long exposure) and at day 3 for the defecation rate (Table 3). Significant changes were recorded at all time points for compound **22** after exposure to the MBC concentration (Table 3). Finally, the developmental timing was found increased by 1.1 h at the MFC and MBC concentrations for compounds **15** and **22**, respectively (Table 3). Thus, our results suggest that compound **22** is more toxic than compound **15** at high concentrations. The observed differences are in accordance with previous studies examining the toxicity of various agents. More specifically, pharyngeal pumping rate and defecation rhythms have been shown to be highly responsive to various toxic agents such as anti-obesity drugs (Reductil® and Xenical®; reduction of pharyngeal pumping rate upon exposure to Reductil® and increase of defecation rate upon exposure to Xenical®; [23]), biochars (increased interval time between two defecations, no impact on the pumping velocity; [24]), soils with various degrees of pollution (significantly reduced pharyngeal pumping velocity; [25]). Developmental delay has been also observed in nematodes after exposure to arsenic, lead and mercury heavy metals [27]. In total, we revealed alterations in our animal populations mainly following exposure to the highest effective concentrations (MFC and MBC) but importantly not to the MIC concentrations. Therefore, our results advocate for rather low toxicity effects of both compounds.

2.4. Computational studies

2.4.1. Insights into the mechanisms of antimicrobial activity

In order to propose a putative mechanism for the antimicrobial activity of the most potent compounds, a two-step computational process was applied, using ligand-based similarity search and molecular docking, in order to predict the binding of the active candidates to the target receptor of similar antibiotics [28,29].

In the case of antibacterial activity, the similarity metrics analysis indicates that the most potent synthetic derivatives (compounds **14** and **22** - query molecule) present fingerprint similarity with the known FDA-approved drug Levofloxacin [30], a broad-spectrum, third-generation fluoroquinolone antibiotic. It is well known that Levofloxacin diffuses through the bacterial cell wall and its activity is through inhibition of bacterial topoisomerase II DNA gyrase, an enzyme required for bacterial DNA replication and repair as well as RNA transcription. Overall, its inhibition blocks the bacterial cell growth. Taking this observation into account, the crystal structure of *S. aureus* gyrase co-crystallized with ciprofloxacin was selected for further docking studies (PDB ID:2XCT) [31].

Similarly, querying compound **15** (the most potent antifungal analogue) revealed itraconazole, a first generation triazole antifungal drug, among the structurally similar compounds. Itraconazole inhibits the synthesis of fungal sterols by inhibiting the cytochrome P450-dependentlanosterol 14α-demethylase (CYP51A) enzyme [32]. The referred enzyme plays a crucial role in the biosynthesis of ergosterol

Table 2
In vitro antifungal evaluation of compounds **14–16, 18–20, 22–25** and **31–33**.

Compounds	MIC/MFC (mM)								
		A. fum.	*A.v.*	*A.o.*	*A.n.*	*T.v.*	*P. f.*	*P.o.*	*P.v.c.*
14	**MIC**	0.013 ± 0.03^{a}	0.013 ± 0.03^{a}	0.026 ± 0.004^{b}	0.026 ± 0.004^{c}	0.026 ± 0.004^{b}	0.026 ± 0.004^{b}	0.026 ± 0.004^{b}	0.013 ± 0.03^{a}
	MFC	0.416 ± 0.03^{c}	0.208 ± 0.005^{c}	0.208 ± 0.005^{c}	0.208 ± 0.005^{c}	0.208 ± 0.005^{c}	0.208 ± 0.005^{c}	0.208 ± 0.005^{c}	0.208 ± 0.005^{c}
15	**MIC**	**0.027** ± 0.005^{a}	**0.027** ± 0.005^{b}	**0.027** ± 0.005^{b}	**0.027** ± 0.005^{b}	**0.027** ± 0.005^{b}	**0.027** ± 0.005^{b}	**0.027** ± 0.005^{b}	**0.027** ± 0.005^{b}
	MFC	**0.056** ± 0.005^{a}	**0.056** ± 0.005^{a}	**0.058** ± 0.005^{a}	**0.056** ± 0.005^{a}	**0.056** ± 0.005^{a}	**0.056** ± 0.005^{a}	**0.056** ± 0.005^{a}	**0.056** ± 0.005^{a}
16	**MIC**	0.210 ± 0.03^{d}	0.045 ± 0.03^{c}	0.027 ± 0.01^{b}	0.105 ± 0.02^{d}	0.027 ± 0.01^{b}	0.027 ± 0.01^{b}	0.027 ± 0.01^{b}	0.045 ± 0.03^{c}
	MFC	0.420 ± 0.06^{c}	0.056 ± 0.03^{a}	0.056 ± 0.03^{a}	0.21 ± 0.02^{c}	0.056 ± 0.03^{a}	0.056 ± 0.03^{a}	0.056 ± 0.03^{a}	0.056 ± 0.03^{a}
18	**MIC**	0.233 ± 0.03^{d}	0.012 ± 0.01^{a}	0.015 ± 0.008^{a}	0.015 ± 0.008^{a}	0.015 ± 0.008^{a}	0.015 ± 0.008^{a}	0.015 ± 0.008^{a}	0.015 ± 0.008^{a}
	MFC	0.465 ± 0.04^{d}	0.233 ± 0.08^{c}	0.233 ± 0.05^{c}	0.233 ± 0.05^{c}	0.233 ± 0.05^{c}	0.233 ± 0.05^{c}	0.233 ± 0.05^{c}	0.232 ± 0.05^{c}
19	**MIC**	0.057 ± 0.005^{b}	0.029 ± 0.003^{b}	0.029 ± 0.005^{b}	0.029 ± 0.005^{b}	0.029 ± 0.005^{b}	0.029 ± 0.005^{b}	0.029 ± 0.005^{b}	0.225 ± 0.025^{e}
	MFC	0.112 ± 0.02^{b}	0.059 ± 0.003^{a}	0.06 ± 0.015^{a}	0.05 ± 0.015^{a}	0.06 ± 0.015^{a}	0.06 ± 0.015^{a}	0.06 ± 0.015^{a}	0.45 ± 0.05^{d}
20	**MIC**	0.926 ± 0.14^{c}	0.464 ± 0.02 ^{g}	0.232 ± 0.02^{d}	0.464 ± 0.02^{e}	0.059 ± 0.01^{c}	0.059 ± 0.01^{c}	0.059 ± 0.01^{c}	0.464 ± 0.02^{f}
	MFC	1.852 ± 0.20^{e}	0.926 ± 0.14^{f}	0.464 ± 0.02^{d}	0.926 ± 0.14^{e}	0.464 ± 0.02^{d}	0.464 ± 0.02^{d}	0.464 ± 0.02^{d}	0.926 ± 0.14^{e}
22	**MIC**	0.065 ± 0.03^{b}	0.034 ± 0.002^{bc}	0.034 ± 0.01^{b}	0.065 ± 0.03^{c}	0.034 ± 0.01^{b}	0.065 ± 0.03^{c}	0.034 ± 0.01^{bc}	0.065 ± 0.03^{d}
	MFC	0.259 ± 0.06^{bc}	0.259 ± 0.04^{c}	0.13 ± 0.03^{b}	0.129 ± 0.02^{b}	0.065 ± 0.03^{a}	0.13 ± 0.02^{b}	0.065 ± 0.03^{a}	0.259 ± 0.03^{c}
23	**MIC**	0.046 ± 0.01^{a}	0.046 ± 0.06^{c}	0.046 ± 0.01^{bc}	0.041 ± 0.01^{bc}	0.046 ± 0.01^{bc}	0.046 ± 0.01^{bc}	0.046 ± 0.01^{c}	0.046 ± 0.01^{c}
	MFC	0.095 ± 0.03^{b}	0.095 ± 0.02^{b}	0.095 ± 0.03^{ab}	0.095 ± 0.03^{b}	0.095 ± 0.03^{b}	0.095 ± 0.03^{b}	0.095 ± 0.03^{b}	0.095 ± 0.03^{b}
24	**MIC**	0.063 ± 0.003^{b}	NA	NA	0.125 ± 0.003^{d}	NA	NA	NA	0.125 ± 0.003^{de}
	MFC	2.00 ± 0.40^{e}	NA	NA	0.501 ± 0.05^{d}	NA	NA	NA	1.001 ± 0.05 ^{e}
25	**MIC**	1.980 ± 0.67^{f}	0.98 ± 0.067^{d}	0.99 ± 0.08^{c}	1.32 ± 0.30^{f}	0.55 ± 0.00^{d}	0.55 ± 0.00^{c}	0.55 ± 0.00^{c}	1.98 ± 0.10 ^{h}
	MFC	3.960 ± 1.12^{f}	1.98 ± 0.10 ^{g}	1.98 ± 0.10^{f}	1.98 ± 0.10^{f}	1.98 ± 0.10^{f}	3.96 ± 0.30 ^{g}	3.96 ± 0.30 ^{h}	3.96 ± 0.30 ^{g}
31	**MIC**	0.171 ± 0.06 ^{cd}	0.044 ± 0.02^{c}	0.109 ± 0.08^{c}	0.171 ± 0.06^{d}	0.044 ± 0.02^{bc}	0.044 ± 0.02^{bc}	0.044 ± 0.02^{c}	0.171 ± 0.06^{e}
	MFC	1.363 ± 0.30^{d}	0.171 ± 0.06^{bc}	0.171 ± 0.06^{b}	0.342 ± 0.02 ^{cd}	0.171 ± 0.06^{bc}	0.342 ± 0.02 ^{cd}	0.342 ± 0.02^{d}	0.342 ± 0.02 ^{cd}
32	**MIC**	0.433 ± 0.03^{e}	0.035 ± 0.005^{bc}	0.021 ± 0.01^{ab}	0.443 ± 0.03^{e}	0.035 ± 0.005^{b}	0.443 ± 0.03^{e}	0.443 ± 0.03^{d}	0.443 ± 0.03^{f}
	MFC	3.188 ± 0.90^{f}	0.044 ± 0.04^{a}	0.044 ± 0.04^{a}	0.797 ± 0.03^{de}	0.044 ± 0.02^{a}	0.797 ± 0.03^{e}	0.797 ± 0.03^{e}	3.188 ± 0.90 ^{g}
33	**MIC**	0.227 ± 0.03^{d}	0.227 ± 0.03^{e}	0.227 ± 0.03^{d}	0.455 ± 0.05^{e}	0.057 ± 0.005^{c}	0.057 ± 0.005^{c}	0.455 ± 0.05^{d}	0.455 ± 0.05^{f}
	MFC	1.820 ± 0.50^{e}	0.455 ± 0.05^{d}	0.455 ± 0.05^{d}	0.91 ± 0.01^{e}	0.455 ± 0.05^{d}	0.901 ± 0.05^{f}	1.82 ± 0.025^{f}	1.82 ± 0.025^{f}
Ketoconazole	**MIC**	0.376 ± 0.004^{de}	0.376 ± 0.004^{f}	0.282 ± 0.04^{d}	0.376 ± 0.004^{e}	1.882 ± 0.07^{e}	0.376 ± 0.004^{d}	1.882 ± 0.07^{f}	2.882 ± 0.50 ^{h}
	MFC	0.941 ± 0.03^{d}	0.941 ± 0.03^{f}	0.376 ± 0.004 ^{cd}	0.941 ± 0.03^{e}	2.822 ± 0.50 ^{g}	0.941 ± 0.03^{f}	2.882 ± 0.50 ^{g}	3.763 ± 0.60 ^{g}
Bifonazole	**MIC**	0.483 ± 0.01^{e}	0.332 ± 0.04^{f}	0.483 ± 0.01^{e}	0.483 ± 0.01^{e}	0.483 ± 0.01^{d}	0.644 ± 0.07^{f}	0.644 ± 0.07^{e}	0.644 ± 0.07 ^{g}
	MFC	0.644 ± 0.07 ^{cd}	0.644 ± 0.07^{e}	0.644 ± 0.07^{e}	0.644 ± 0.07^{de}	0.644 ± 0.07^{e}	0.805 ± 0.06^{e}	0.805 ± 0.07^{e}	0.966 ± 0.08^{e}

NA: not active.
A.fum.: A. fumigatus, A.v.: A. versicolor, A.o.: A. ochraceus, A.n.: A. niger, T.v.: T. viride, P.f.: P. funiculosum, P.o.: P. ochrochloron, P.v.c.: P. verrucosum var. *cyclopium.*
Values are expressed as means ± SD. Different letters in each column indicate statistically significant differences between samples ($p < 0.05$).

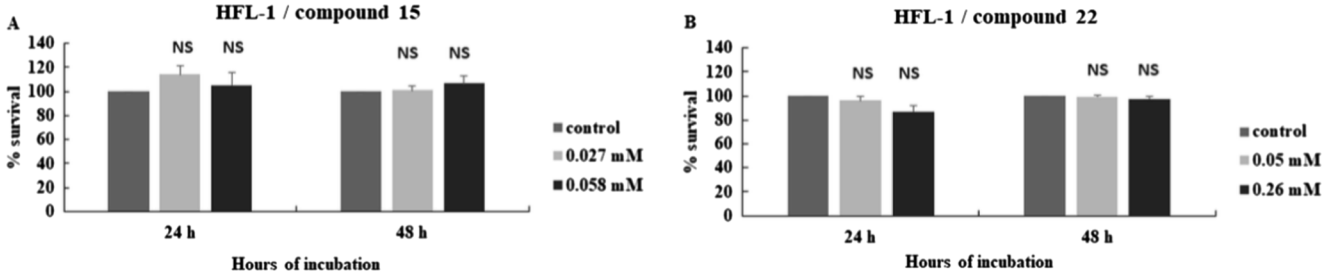

Fig. 2. Absence of toxic effects of compounds **15** and **22** in HFL-1 human primary cells. Survival ratio following crystal violet staining of HFL-1 human embryonic primary fibroblasts treated with (A) 0.027 and 0.058 mM compound **15** and B) 0.05 and 0.26 mM compound **22** or the appropriate amount of DMSO (control) for 24 and 48 h. The dye absorbance exhibited by the control cells was set to 100%. All values are reported as mean of three independent experiments. Error bars denote ± SEM. NS (not significant).

catalyzing the demethylation step of lanosterol to ergosterol. Due to the absence of crystal structures of CYP51A enzyme of the examined fungi, a previously published homology model of *A. fumigatus* was used for docking studies [33].

The docking results of compounds **14** and **22** on *S. aureus* topoisomerase II DNA gyrase present Glide scores (−7.2 and −7.1 kcal·mol^{-1} respectively), in the range of previously reported active antibacterials [34] as well as interactions with enzyme residues and DNA bases at the active site of the enzyme. Specifically, compound **22** interacts similarly to ciprofloxacin and levofloxacin [30] with the crucial residue Ser1084 through H bond formation and with DG8 and DG9 DNA chains through π-π interactions. Additionally, it's binding pose interacts with the amino acid Arg1122 through a π-cation interaction. (Fig. 3B, Table 4). Finally, the amine group of compound **22** is located in close proximity with the Mn cation although metal chelation interactions were not conserved in all docked poses.

The binding poses of compound **14** are also located in the active site of the enzyme interacting through π-π interactions and hydrogen bonds with the DG8 and DG9 DNA chains, but lacks the interaction with the amino acid Ser1084. Interestingly, it seems to interact with Asp437 through halogen bond, a residue also found in contact with the bound pose of levofloxacin in previous studies [30] (Fig. 3A, Table 4).

The docking results of compounds **14** and **15** present Glide scores −8.6 ·and −8.1 kcal mol^{-1} respectively with both compounds being

Table 3
Phenotypic analysis of *C. elegans* N2 wt strain treated with compounds **15** and **22** or DMSO (control) at day 1 and 3 of adulthood.

	DAY 1			DAY 3		
	Concentration (mM)	**Pharyngeal pumping** [a]	**Defecation** [b]	**Pharyngeal pumping** [a]	**Defecation** [b]	**Developmental timing** [c]
DMSO (**15**)		225.3 ± 4.5	47.4 ± 1.1	199.3 ± 3.4	51.2 ± 0.7	52.4 ± 0.36
Compound **15**	0.027	222.4 ± 3.0	47.2 ± 0.7	195.3 ± 2.4	51.6 ± 0.6	53.4 ± 0.22
	0.058	182.2 ± 3.6***	46.3 ± 0.5	204.4 ± 1.8	44.8 ± 0.7***	53.5 ± 0.20*
DMSO (**22**)		213.6 ± 1.7	43.8 ± 0.4	212.7 ± 1.3	52.6 ± 0.5	52.8 ± 0.18
Compound **22**	0.05	214.7 ± 4.5	45.6 ± 0.8*	200.4 ± 2.2***	51.2 ± 0.8	53.6 ± 0.22
	0.26	176.7 ± 2.1***	47.4 ± 0.4***	203.2 ± 1.9***	57.9 ± 0.5***	53.9 ± 0.22**

All assays were performed at 20 °C. The results are presented as mean (n = 3) ± SEM.
***p < 0.001,**p < 0.005, *p < 0.05 as compared to DMSO.
[a] Number of Pumps in 1 min at day 1 and 3 of adulthood.
[b] Duration of defecation cycle in seconds at day 1 and 3 of adulthood.
[c] Duration of post-embryonic development (hours from egg hatching to L4 moult).

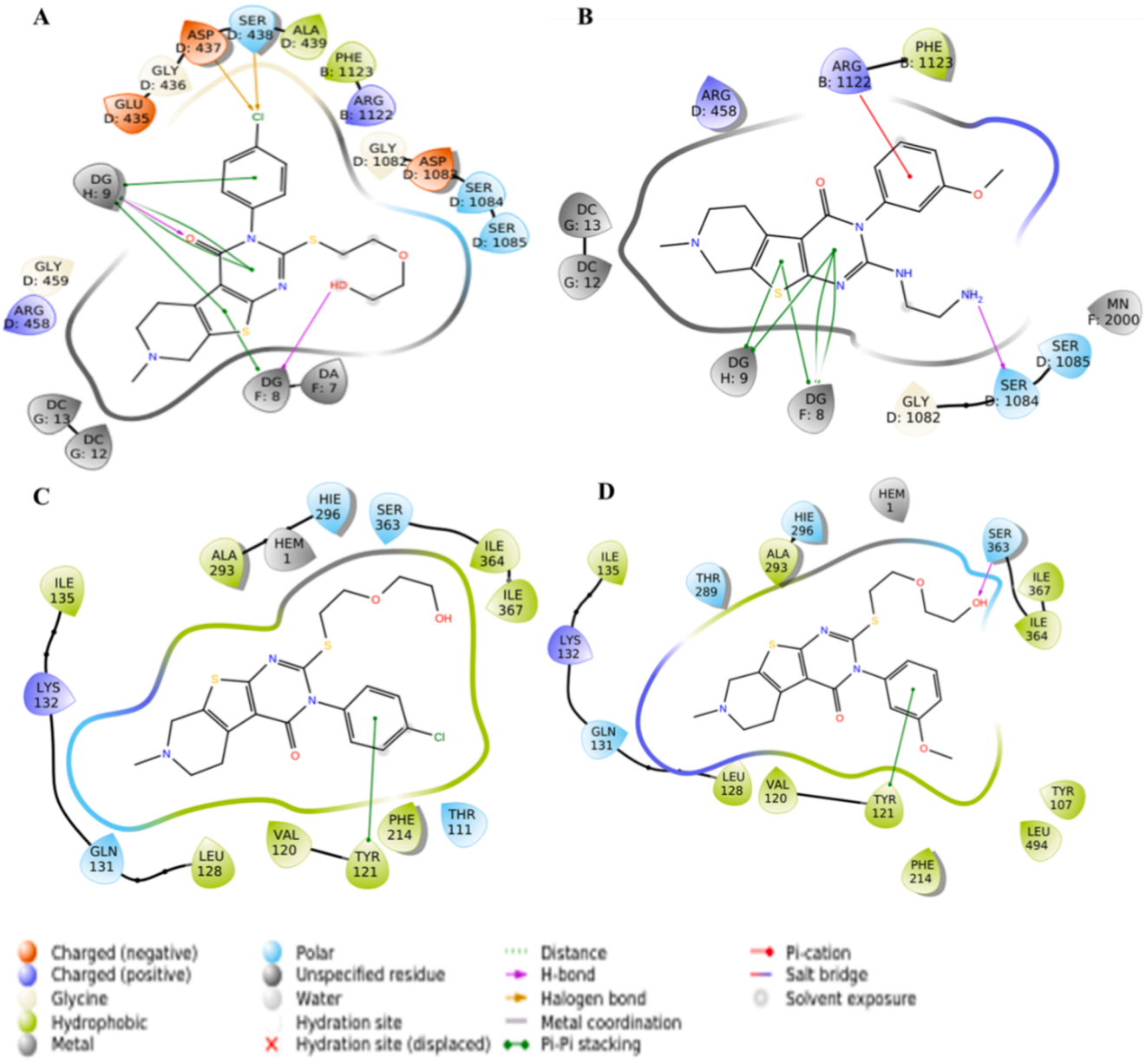

Fig. 3. 2D protein- ligand interaction diagrams of (A) compound **14** (docking score = −7.2 kcal·mol^{-1}) and (B) compound **22** (docking score = −7.1 kcal·mol^{-1}) into the active site of *S. aureus* topoisomerase II DNA gyrase (PDB ID:2XCT) and (C) compound **14** (docking score = −8.6 kcal·mol^{-1}) and (D) **15** (docking score = −8.1 kcal·mol^{-1}) into the active site of *A. fumigatus* CYP51A enzyme [33].

Table 4
Docking interactions with *S. aureus* topoisomerase II DNA gyrase enzyme.

Protein Residues / DNA bases	Ciprofloxacin	Compound 14	Compound 22
Mn^{2+}	Chelation	–	Contact/ chelation
Ser1084	H-bond	–	H-bond
Arg1122	–	–	π-cation
Asp437 / Ser438	–	Halogen bond	–
DG8	π-π & π-cation	π-π & H-bond	π-π
DG9	π-π & π-cation	π-π & H-bond	π-π
DC13	H-bond	Contact	Contact

positioned into the *A. fumigatus* CYP51A active site. Docking poses reveal a binding mode similar to R-econazole, with formation of π-π interactions with Tyr121, a consistent amino acid interaction found in azole family of CYP51A inhibitors [33]. Furthermore, the hydroxyl group of compound **15** forms an H-bond with Ser363, a residue also noted to contribute in binding [33]. Finally, the ether oxygen atom of both compounds **14** and **15**, is in proximity with the heme iron atom (Fig. 3C and D, respectively and Table 5).

2.4.2. Computational model for structure activity relationship analysis

In order to obtain a better understanding about the structure activity relationships a Pharma QSAR model was developed based on scaffold decomposition and R-group analysis (Materials and methods section). Specifically, the 13 studied compounds were subjected to scaffold decomposition to identify common structural features (core structural motifs). Although the pyrimidinone ring (Fig. 4A) was found as a common scaffold among all the synthesized compounds, it cannot provide satisfactory SAR results since it is a generic core with many and different substitutions. At a step further, a core scaffold consisting of a thienopyrimidinone ring substituted with a phenyl and a *N*-methylpiperidine ring was selected (Fig. 4B) which is encountered in 10 out of 13 compounds. Subsequently, R-group analysis was performed to identify the attachment points on the core scaffold, (R-groups), and their correlation with the molecular properties.

The correlation of the R-groups (based on their pharmacophore features) with the *in vitro* antibacterial activity (MIC values) for each bacterial species is presented in Table 6 and Fig. S2 (Supplementary Material). Some general observations can be drawn from the results. The presence of a hydrogen bond acceptor (HB-A) or a hydrophobic group (H) at R_1 position have a negative impact in almost all bacterial strains with the exception of *L. monocytogenes* and *E. coli* (i.e. compounds **22** and **24**). Furthermore, a hydrophobic substituent is preferred at R_2 position except for the cases of *L. monocytogenes* and *E. coli* while, a hydrogen bond acceptor (HB-A) at R_2 is beneficial for *M. flavus E. coli* and *En. cloacae* (i.e. compounds **16** and **19**). Thus, among compounds **14**, **15** and **16**, the methoxy (-OMe) substitution at *meta* position (R_1) of compound **15** caused a significant decrease in activity compared to compound **14** bearing the same (-OMe) group at the *para* position (R_2) of the phenyl ring (Table 6). Substitution of the methoxy group with a chlorine (-Cl) atom (as in the case of compound **16**) exhibited one-fold increase of the activity against *E. coli*. With respect to R_4 position, a hydrogen bond donor (HB-D) is clearly preferred for most species, while, the HB-A at R_4 positively affects the species of *B. cereus*, *S. aureus, En. cloacae* and *S. typhimurium*. Finally, hydrophobic groups at R_4 negatively affect *M. flavus*, *L. monocytogenes*, *E. coli* and *S. typhimurium* (i.e. compound **25**). Comparing compounds **22**, **24** and **25** which all bear HB-D or HB-A at R_4, the ethylene diamine side chain of compound **22** significantly reinforces its antibacterial activity in all tested strains compared to compounds **24** and **25**, indicating as optimal the two-carbon atom chain. In contrast, the addition of one more carbon in the side chain induces a reduction in the activity while the replacement by a piperazine ring leads to a complete loss of antibacterial activity. Finally, the effect of R_3 substitutions could not be evaluated since all tested compounds bear a methyl group.

Table 5
Docking interactions with *A. fumigatus* CYP51A enzyme.

Protein Residues	Econazole	Compound 14	Compound 15
Fe^{3+}	Chelation	Contact	Contact
Tyr107	π-π	–	–
Tyr121	π-π	π-π	π-π
Ser363	–	–	*H-bond*

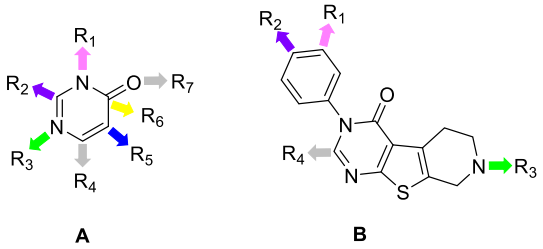

Fig. 4. (A) The pyrimidinone ring as a common scaffold of the synthesized compounds, and (B) the selected core scaffold including a thienopyrimidinone ring substituted with a phenyl and a *N*-methylpiperidine ring. The attachment positions are designated as Rs.

Similar models were generated to correlate the antifungal activity with the pharmacophore features of the new compounds. Statistical models were generated focusing on the previous core scaffold, offering a putative explanation of compounds' antifungal activity against *A. fumigatus, A. niger* and *P. verrucosum* var. *cyclopium* (Table 7A, Fig. S3, Supplementary Material). Since compound **24** was completely inactive against *A. versicolor, A. ochraceus, T. viride, P. funiculosum* and *P. ochrochloron*, it was excluded from the dataset and models were re-generated (Table 7B).

The Pharma RQSAR models indicate that the presence of a hydrogen bond acceptor (HB-A) or a hydrophobic (H) group at R_1 position has a negative effect on activity against *A. niger* (i.e. compound **24**), while this is not observed for the cases of *A. fumigatus* and *P. verrucosum* var. *cyclopium*. Regarding the R_2 position, a hydrophobic (H) substituent results into a positive effect on activity against *A. niger* (i.e. compounds **18** and **19**) while again *A. fumigatus* and *P. verrucosum* var. *cyclopium* are not affected by substitutions at R_2 (similarly to R_1). Regarding the R_4 position, a hydrogen bond acceptor (HB-A) leads to increase of activity against *A. niger, A. fumigatus* and *P. verrucosum* var. *cyclopium* species. Substitution by an HB-D increases the antifungal activity against *A. niger* and *P. verrucosum* var. *cyclopium* species. (i.e. compounds **14** and **15**).

Specifically, a comparison between compounds **14** and **16**, sharing a common substitution at R_4, indicated the crucial role of chlorine (-Cl) at R_2 position which is reflected by the strongest antifungal activity of compound **14**. Comparison of compounds **18**, **19** and **20**, bearing a common chlorine (-Cl) atom at R_2 position, showed a stronger antifungal activity for compounds **18** and **19** compared to **20** which may be explained by the replacement of the terminal amino group of the aliphatic amines by a hydroxyl group at R_4 position.

According to the second model for *A. versicolor, A. ochraceus, T. viride, P. funiculosum* and *P. ochrochloron* (Fig. S4, Supplementary Material), common SAR patterns are observed for all species (Table 7). Specifically, a substitution at R_1 position with an HB-A or a hydrophobic (H) group (compound **15**) negatively affects the activity while hydrophobic (H) groups at R_2 position (compounds **14**, **18** and **19**) induce a positive effect. Moreover, a hydrogen bond acceptor (HB-A) at R_4 position positively affects antifungal activity (compounds **18**, **19** and **22**). Indicatively, comparison between compounds **22** and **25** proved that in the case of compound **22** the ethylenediamine side chain at R_4 position contributes positively to antifungal activity while its replacement by the piperazine moiety (compound **25**) leads to loss of activity.

Table 6
Effect of substituents on antibacterial activity as derived from the Pharma RQSAR models.

	Attachment Positions – Activity Effect						
	R_1		R_2		R_4		
Bacterial strains	**HB-A**	**H**	**HB-A**	**H**	**HB-D**	**HB-A**	**H**
B. cereus	Negative	Negative	Weak	Positive	Positive	Positive	Weak
M. flavus	Negative	Negative	Positive	Positive	Positive	Weak	Negative
S. aureus	Negative	Negative	Weak	Positive	Positive	Positive	Weak
L. monocytogenes	Weak	Weak	Weak	Weak	Positive	Weak	Negative
E. coli	Weak	Weak	Positive	Weak	Positive	Weak	Negative
En. cloacae	Negative	Negative	Positive	Positive	Weak	Positive	Weak
P. aeruginosa	Negative	Negative	Weak	Positive	Positive	Weak	Weak
S. typhimurium	Negative	Negative	Weak	Positive	Positive	Positive	Negative

Attachment positions: R_1 (meta) - R_2 (ortho) substituted phenyl ring is attached at the *N*-3 position of the thieno[2,3-*d*]pyrimidin-4(3*H*) scaffold, R_4 aliphatic amines or alcohols are anchored at the C-2 position through a sulfur or amino bridge. Pharmacophore features representation: Hydrogen bond acceptor (HB-A), Hydrogen bond donor (HB-D), Hydrophobic region (H).

Table 7
Effect of substituents on the antifungal activity as derived from the Pharma RQSAR models.

	Attachment Positions – Activity Effect						
Fungal strains	R_1		R_2		R_4		
1st model (Table 7A)							
	HB-A	**H**	**HB-A**	**H**	**HB-D**	**HB-A**	**H**
A. fumigatus	Weak	Weak	Weak	Weak	Weak	Positive	Positive
A. niger	Negative	Negative	Weak	Positive	Positive	Positive	Weak
P. cycl.	Weak	Weak	Weak	Weak	Positive	Positive	Weak
2nd model (Table 7B)							
A. ochraceus	Negative	Negative	Weak	Positive	Weak	Positive	Weak
A. versicolor	Negative	Negative	Weak	Positive	Weak	Positive	Positive
P. funiculosum	Negative	Negative	Weak	Positive	Weak	Positive	Weak
P. ochrochloron	Negative	Negative	Weak	Positive	Weak	Positive	Weak
T. viride	Negative	Negative	Weak	Positive	Weak	Positive	Weak

Attachment positions: R_1 (meta) - R_2 (ortho) substituted phenyl ring is attached at the *N*-3 position of the thieno[2,3-*d*]pyrimidin-4(3*H*) scaffold, R_4 aliphatic amines or alcohols are anchored at the C-2 position through a sulfur or amino bridge. Pharmacophore features representation: Hydrogen bond acceptor (HB-A), Hydrogen bond donor (HB-D), Hydrophobic region (H).

Finally, the molecular properties of the synthesized compounds were calculated indicating that they are within the ranges of the recommended values for drug likeliness (Table S3, Supplementary Material).

3. Conclusions

A series of new thieno[2,3-*d*]pyrimidin-4(3*H*)-one derivatives were synthesized and evaluated for their activity against four gram-positive and four gram-negative bacterial strains and eight fungal species. The structural variations included substitution at *N*-3 position by a phenyl ring bearing an electron-donating (-OMe) or electron-withdrawing (-Cl) group, biocompatible aliphatic amines or a hydroxyalkoxy group anchored at the C-2 position through a sulfur or amino bridge and a *N*-methylpiperidine or a cyclohexane moiety fused to the thieno[2,3-*d*] pyrimidin-4(3*H*)-one core.

The majority of the compounds exhibited excellent antimicrobial and/or antifungal activity, being more potent than the control compounds.

The most potent antibacterial agent was compound **22**, bearing at *N*-3 a *m*-methoxyphenyl group and an ethylenediamine side chain at C-2, presenting broad spectrum activity with MIC = 0.027 ± 0.005 mM and MFC = 0.056 ± 0.005 mM against all strains tested. The most potent antifungal agent was **15** substituted by a *m*-methoxyphenyl group at *N*-3 and a 2-(2-mercaptoethoxy)ethan-1-ol side chain at C-2 with MIC = 0.027 ± 0.005 mM and MFC = 0.056 ± 0.005 mM against all fungal strains tested. Furthermore, compound **22** also showed high antifungal potency with MIC values ranging between 0.034 and 0.065 mM and MFC ranging between 0.065 and 0.259 mM. Evaluation of the potential toxic effects of compounds **15** and **22** *in vitro* on HFL-1 human embryonic primary cells and *in vivo* on the nematode *C. elegans*, revealed absence of *in vitro* toxicity at MIC/MFC and MIC/MBC concentrations, and of *in vivo* toxicity at MIC concentrations for both compounds.

Furthermore, R-Group analysis as a means of structure activity relationships computational tool, highlighted the effect of specific chemical features (as substituents on a core scaffold) on the antibacterial and antifungal activity.

Finally, a putative mechanism of antibacterial activity is related to inhibition of the topoisomerase II DNA gyrase enzyme as shown for the case of *S. aureus* and the active analogue **22**, while inhibition of CYP51 lanosterol demethylase enzyme may be a putative mechanism for antifungal activity as presented for the case of *A. fumigatus* and compound **15**.

In conclusion, compounds **15** and **22** represent promising leads for the further development of potent antimicrobial and antifungal agents and future studies are required to optimize their efficacy against additional strains including resistant ones and to delineate the mechanism(s) of their activity.

4. Experimental

4.1. Chemistry

Melting points were determined with a Buchi 510 apparatus and are uncorrected. ^{1}H NMR spectra were recorded on Varian spectrometers operating at 300 MHz or 600 MHz and ^{13}C NMR spectra were recorded at 75 MHz or 150 MHz respectively. Chemical shifts are reported in δ units, parts per million (ppm) downfield from TMS. IR spectra were recorded by using the attenuated total reflection (ATR) method on a

FTIR Bruker Tensor 27. Electro-spray ionization (ESI) mass spectra were recorded on a LC-MS^n Fleet, Thermo spectrometer using MeOH as solvent. HRMS spectra were recorded, in the ESI mode, on UPLC-MSn Orbitrap Velos-Thermo. Reactions under microwave irradiation were performed in a CEM Discover Lab Mate reactor. Flash column chromatography (FCC) was performed on Merck silica gel 60 (230–400 mesh) and TLC on Merck 60 F254 films (0.2 mm) precoated glass plates. Spots were visualized with UV light at 254 nm and ninhydrin or PMA stain. All solvents were dried and/or purified according to standard procedures prior to use. All reagents employed in the present work were purchased from commercial suppliers and used without further purification. Reactions were run in flame-dried glassware under an atmosphere of argon.

*4.1.1. Ethyl 2-amino-6-methyl-4,5,6,7-tetrahydrothieno[2,3-c]pyridine-3-carboxylate (**3**)*

To an ice-cold rb-flask containing *N*-methyl-4-piperidone (**1**) (2.87 mL, 25.0 mmol), sulfur (0.8 g, 25.0 mmol) and ethyl cyanoacetate (**2**) (2.66 mL, 25.0 mmol), a solution of diethylamine (2.57 mL, 25.0 mmol) in MeOH (2 mL) was added. Then, a condenser was installed and irradiated for 4 min at 120 W and 100 °C in a CEM-Discover microwave reactor. The reaction mixture was cool to room temperature and then diluted with DCM (50 mL). The organic layer was washed with brine (30 mL), dried over anhydrous Na_2SO_4 and concentrated under reduced pressure. The residue was recrystallized using MeOH/diethyl ether/hexane to afford compound **3** as a brownish solid (4.2 g, 69%); $R_f = 0.30$ (DCM/MeOH 95:5); m.p: 82–84 °C; ^{1}H NMR (300 MHz, $CDCl_3$): δ 4.26 (q, $J = 7.1$ Hz, 2H), 3.38 (s, 2H), 2.84 (t, $J = 5.9$ Hz, 2H), 2.66 (t, $J = 5.9$ Hz, 2H), 2.44 (s, 3H), 1.33 (t, $J = 7.1$ Hz, 3H); ^{13}CNMR (75 MHz, $CDCl_3$): δ 165.9, 162.0, 130.6, 114.5, 105.3, 59.5, 53.3, 52.4, 45.4, 27.3, 14.4; ESI-MS: *m/z* 241 $[M+H]^+$.

*4.1.2. General procedure for the preparation of compounds **7**–**9***

In a 10 mL microwave reaction tube, compound **3** (0.3 g, 1.25 mmol) and the corresponding aryl isothiocyanate **4**, **5** or **6** were mixed (3 mL of dry pyridine was also added in the case of compound **4**). The tube was sealed and irradiated in a CEM Discover microwave reactor at 120 W, 100 °C, over 2 min. After cooling at ambient temperature the residues were subjected to FCC to afford the desired compounds in pure form. In the case of **4** pyridine was evaporated under reduced pressure first and the residue was subjected to FCC to afford the desired compound in pure form.

*4.1.2.1. Ethyl 2-(3-(4-chlorophenyl)thioureido)-6-methyl-4,5,6,7-tetrahydrothieno [2,3-c]pyridine-3-carboxylate (**7**).* Using the general procedure above compound **3** (0.3 g, 1.25 mmol), 4-chlorophenyl isothiocyanate (**7**) (0.32 g, 1.88 mmol) and pyridine (3 mL), the title compound was obtained as a yellow solid (0.256 g, 50%) after FCC (EtOAc/ MeOH, 97:3); $R_f = 0.24$ (DCM/MeOH 95:5); m.p. 204–206 °C (Lit. [35] – 206–208 °C); ^{1}H NMR (300 MHz, $CDCl_3$): δ 12.21 (s, 1H), 7.84 (s, 1H), 7.43 (d, $J = 8.4$ Hz, 2H), 7.29 (d, $J = 8.4$ Hz, 2H), 4.19 (q, $J = 7.1$ Hz, 2H), 3.51 (s, 2H), 2.87 (t, $J = 5.8$ Hz, 2H), 2.68 (t, $J = 5.8$ Hz, 2H), 2.47 (s, 3H), 1.29 (t, $J = 7.1$ Hz, 3H).

*4.1.2.2. Ethyl 2-(3-(3-methoxyphenyl)thioureido)-6-methyl-4,5,6,7-tetrahydrothieno [2,3-c]pyridine-3-carboxylate (**8**).* Using the general procedure above, compound **3** (0.3 g, 1.25 mmol) and 3-methoxyphenyl isothiocyanate (**8**) (0.22 mL, 1.56 mmol), the title compound was obtained as a yellow solid (0.41 g, 80%) after FCC (EtOAc/MeOH, 97:3); $R_f = 0.42$ (EtOAc/MeOH 9:1); ^{1}H NMR (600 MHz, $CDCl_3$): δ 12.19 (s, 1H), 7.94 (s, 1H), 7.34 (t, $J = 8.4$ Hz, 1H), 6.91–6.85 (m, 3H), 4.14 (q, $J = 7.1$ Hz, 2H), 3.81 (s, 3H), 3.51 (s, 2H), 2.86 (t, $J = 5.7$ Hz, 2H), 2.68 (t, $J = 5.8$ Hz, 2H), 2.47 (s, 3H), 1.25 (t, $J = 7.1$ Hz, 3H); ^{13}C NMR (150 MHz, $CDCl_3$): δ 175.9, 166.0, 160.7, 150.5, 136.7, 130.7, 128.9, 123.4 117.2, 113.9, 112.5, 110.5, 60.5, 55.4, 53.0, 52.3, 45.3, 26.6, 14.1.

*4.1.2.3. Ethyl 2-(3-(4-methoxyphenyl)thioureido)-6-methyl-4,5,6,7-tetrahydrothieno [2,3-c]pyridine-3-carboxylate (**9**).* Using the general procedure above, compound **3** (0.3 g, 1.25 mmol), 4-methoxyphenyl isothiocyanate (**9**) (0.21 mL, 1.56 mmol) the title compound was obtained as a yellow solid (0.23 g, 45%) after FCC (EtOAc/MeOH, 97:3); $R_f = 0.62$ (DCM/MeOH 9:1); ^{1}H NMR (300 MHz, $CDCl_3$): δ 11.96 (s, 1H), 7.70 (s, 1H), 7.24 (d, $J = 8.8$ Hz, 2H), 6.98 (d, $J = 8.8$ Hz, 2H), 4.12 (q, $J = 7.1$ Hz, 2H), 3.85 (s, 3H), 3.50 (s, 2H), 2.85 (t, $J = 5.9$ Hz, 2H), 2.66 (t, $J = 5.8$ Hz, 2H), 2.46 (s, 3H), 1.24 (t, $J = 7.1$ Hz, 3H).

*4.1.3. 2-(2-hydroxyethoxy)ethyl 4-methylbenzenesulfonate (**13**)*

To a solution of diethylene glycol (7.1 mL, 74.8 mmol) in THF (2.2 mL) a solution of NaOH (0.43 g, 10.85 mmol) in H_2O (2 mL) was added. The mixture was cooled at 0 °C and a solution of *p*-toluenesulfonyl chloride (1.38 g, 7.2 mmol) in THF (2.0 mL) was added dropwise. After stirring for 2 h at rt, the reaction mixture was partitioned between cold water (20 mL) and DCM (30 mL). The organic layer was separated and the aqueous layer was then extracted with DCM (2 × 30 mL). The combined organic layers were washed with brine, dried over Na_2SO_4 and evaporated under reduced pressure to afford the crude title compound **13** which was dried over P_2O_5 for 3 h under high vacuum and used to the next step without further purification. Colourless oil (1.19 g, 63%). $R_f = 0.27$ (petroleum ether/EtOAc 1:1); ^{1}H NMR (300 MHz, $CDCl_3$): δ 7.78 (d, $J = 7.9$ Hz, 2H), 7.34 (d, $J = 8.1$ Hz, 2H), 4.19 (t, $J = 4.5$ Hz, 2H), 3.74–3.59 (m, 4H), 3.52 (t, $J = 4.4$ Hz, 2H), 2.44 (s, 3H), 1.96 (s, 1H).

*4.1.4. General procedure for the preparation of compounds **14**–**16***

To a solution of compound **7**, **8** or **9** (0.46 mmol), an ethanolic KOH solution (2 mL, 0.21 M) was added and the reaction mixture heated to reflux. The progress of the reaction was monitored by TLC. Upon completion, the reaction mixture was filtered and to the filtrate containing the corresponding thiolate **10**–**12**, 2-(2-hydroxyethoxy)ethyl 4-methylbenzenesulfonate (**13**) (0.143 g, 0.55 mmol) was added and the reaction was further heated to reflux for 18 h. The solvent was evaporated under reduced pressure and the projected compounds were isolated in pure form after FCC.

*4.1.4.1. 3-(4-Chlorophenyl)-2-[2-(2-hydroxyethoxy)ethylsulfanyl]-7-methyl-5,6,7,8-tetrahydro-3H-pyrido[4′,3′:4,5]thieno[2,3-d]pyrimidin-4-one (**14**).* Using the general procedure above from compound **7** (0.209 g, 0.46 mmol) the title compound **14** was obtained as a yellow solid (0.13 g, 63%) after FCC (EtOAc/MeOH, 95:5). $R_f = 0.53$ (DCM/MeOH, 9:1); m.p: 180 – 182 °C; IR: 3371, 2939, 1676, 1510 cm^{-1}; ^{1}H NMR (600 MHz, $CDCl_3$): δ 7.50 (d, $J = 8.7$ Hz, 2H), 7.19 (d, $J = 8.7$ Hz, 2H), 3.73 (t, $J = 6.2$ Hz, 2H), 3.70 (dd, $J = 4.8$ and 4.2 Hz, 2H), 3.63 (bs, 2H), 3.57 (dd, $J = 4.8$ and 4.2 Hz, 2H), 3.34 (t, $J = 6.2$ Hz, 2H), 3.06 (t, $J = 5.3$ Hz, 2H), 2.75 (t, $J = 5.3$ Hz, 2H), 2.50 (s, 3H); ^{13}C NMR (150 MHz, $CDCl_3$): δ 162.7, 158.4, 156.9, 136.2, 133.8, 130.3, 130.0, 129.9, 128.7, 118.6, 71.9, 68.8, 61.7, 53.5, 51.8, 45.3, 31.6, 25.7; ESI-MS: *m/z* 452.1 and 454.2 (3:1) $[M+H]^+$; ESI-HRMS: *m/z* $[M+H]^+$ calcd for $C_{20}H_{23}N_3O_3^{35}ClS_2$ 452.0864, found 452.0860.

*4.1.4.2. 2-[2-(2-Hydroxyethoxy)ethylsulfanyl]-3-(3-methoxyphenyl)-7-methyl-5,6,7,8-tetrahydro-3H-pyrido[4′,3′:4,5]thieno[2,3-d]pyrimidin-4-one (**15**).* Using the general procedure above from compound **8** (0.187 g, 0.46 mmol) the title compound **15** was obtained as a yellow gummy solid (0.148 g, 71.5%) after FCC (EtOAc/MeOH, 9:1); $R_f = 0.36$ (EtOAc/MeOH 9:1); IR: 3394, 2919, 1677 cm^{-1}; ^{1}H NMR (300 MHz, $CDCl_3$): δ 7.43 (t, $J = 8.1$ Hz, 1H), 7.05 (ddd, J = 8.1, 2.1 and 0.8 Hz, 1H), 6.85 (ddd, J = 8.1, 2.1 and 0.8 Hz, 1H), 6.79 (t, $J = 2.1$ Hz, 1H), 3.83 (s, 3H), 3.73 (t, $J = 6.3$ Hz, 2H), 3.70 (m, 4H), 3.57 (m, 2H), 3.33 (t, $J = 6.3$ Hz, 2H), 3.09 (t, $J = 6.0$ Hz, 2H), 2.80 (t, $J = 5.8$ Hz, 2H), 2.53 (s, 3H); ^{13}C NMR (75 MHz, $CDCl_3$): δ 162.9, 160.7, 158.6, 157.6, 136.6, 130.6, 129.7, 128.2 121.2, 118.8, 116.1, 114.6, 72.2, 69.1, 61.8, 55.6, 53.6,

52.0, 45.4, 32.3, 25.6; ESI-MS: *m/z* 448.1 $[M+H]^+$; ESI-HRMS: *m/z* $[M+H]^+$ calcd for $C_{21}H_{26}O_4N_3S_2$ 448.1359, found 448.1348.

*4.1.4.3. 2-[2-(2-Hydroxyethoxy)ethylsulfanyl]-3-(4-methoxyphenyl)-7-methyl-5,6,7,8-tetrahydro-3H-pyrido[4′,3′:4,5]thieno[2,3-d]pyrimidin-4-one (**16**).* Using the general procedure above from compound **9** (0.187 g, 0.46 mmol) the title compound **16** was obtained as a light yellow solid (0.124 g, 60%) after FCC (EtOAc/MeOH, 9:1); $R_f = 0.46$ (DCM/MeOH, 9:1); m.p: 124 – 126 °C; IR: 3517, 2918, 1676, 1502 cm^{-1}; ^1H NMR (600 MHz, $CDCl_3$): δ 7.17 (d, $J = 8.9$ Hz, 2H), 7.01 (d, $J = 8.9$ Hz, 2H), 3.85 (s, 3H), 3.72 (t, $J = 6.3$ Hz, 2H), 3.71–3.69 (m, 2H), 3.63 (bs, 2H), 3.57 (t, $J = 5.1$ Hz, 2H), 3.31 (t, $J = 6.3$ Hz, 2H), 3.06 (t, $J = 5.7$ Hz, 2H), 2.75 (t, $J = 5.7$ Hz, 2H), 2.49 (s, 3H); ^{13}C NMR (75 MHz, $CDCl_3$): δ 163.3, 160.7, 159.2, 158.0, 130.2, 129.8, 128.6, 128.1, 118.6, 115.2, 72.1, 69.1, 61.9, 55.7, 53.8, 52.1, 45.6, 32.4, 25.8; ESI-MS: *m/z* 448.1 $[M+H]^+$; ESI-HRMS: *m/z* $[M+H]^+$ calcd for $C_{21}H_{26}O_4N_3S_2$ 448.1359, found 448.1353.

*4.1.5. 3-(4-chlorophenyl)-7-methyl-2-(methylthio)-5,6,7,8-tetrahydropyrido [4′,3′:4,5]thieno[2,3-d]pyrimidin-4(3H)-one (**17**)*

To a rb-flask containing compound **7** (0.16 g, 0.42 mmol), an ethanolic KOH solution (2 mL, 0.21 M) was added and the reaction mixture was heated to reflux until completion of the reaction (monitored by TLC). The reaction mixture was then filtered and a solution of methyl iodide (0.026 mL, 0.42 mmol) in EtOH (1 mL) was added dropwise to the filtrate. The solution was stirred for 90 min and then H_2O (1 mL) was added. The resulting orange precipitate was filtered, washed with H_2O, dried under high vacuum and used in the next step without further purification (0.154 g, 97%). $R_f = 0.69$ (DCM/MeOH, 9:1); ^1H NMR (300 MHz, $CDCl_3$): δ 7.50 (d, $J = 8.6$ Hz, 2H), 7.23 (d, $J = 8.6$ Hz, 2H), 3.84 (bs, 2H), 3.06 (t, $J = 6.0$ Hz, 2H), 2.76 (t, $J = 6.0$ Hz, 2H), 2.50 (s, 3H), 2.49 (s, 3H).

*4.1.6. General procedure for the preparation of compounds **18** and **19***

To a rb-flask, compound **17** (0.102 g, 0.27 mmol) and the appropriate diamine were added and the reaction mixture was stirred at 120 °C for 18 h. Then, the mixture was cooled to rt and passed through a column of neutral aluminium oxide (DCM/MeOH, 8:2). A second purification by FCC on silica gel (DCM/MeOH/25% NH_4OH 6:4:0.5) afforded the desired compounds.

*4.1.6.1. 2-((3-aminopropyl)amino)-3-(4-chlorophenyl)-7-methyl-5,6,7,8-tetrahydropyrido[4′,3′:4,5]thieno[2,3-d]pyrimidin-4(3H)-one (**18**).* Using the general procedure above from compound **17** (0.102 g, 0.27 mmol) and propane-1,3-diamine (0.67 mL, 8.1 mmol) the title compound was obtained as a light-yellow sticky solid (0.054 g, 50%). $R_f = 0.15$ (DCM/MeOH, 8:2); IR: 3407, 2933, 1664, 1546 cm^{-1}; ^1H NMR (600 MHz, CD_3OD): δ 7.64 (d, $J = 8.6$ Hz, 2H), 7.36 (d, $J = 8.6$ Hz, 2H), 4.43 (bs, 2H), 3.58 (bs, 2H), 3.47 (t, $J = 6.6$ Hz, 2H), 3.24 (t, $J = 5.6$ Hz, 2H), 3.05 (s, 3H), 2.97 (t, $J = 6.2$ Hz, 2H), 1.93 (m, 2H); ^{13}C NMR (75 MHz, CD_3OD): δ 167.5, 159.0, 152.0, 135.6, 132.8, 130.62, 130.57, 127.6, 117.4, 112.7, 51.7, 51.1, 42.2, 38.1, 37.1, 27.1, 23.1; ESI-MS: *m/z* 404.07 $[M+H]^+$; ESI-HRMS: *m/z* $[M+H]^+$ calcd for $C_{19}H_{23}N_5OClS$ $[M+H]^+$ 404.1306, found 404.1294.

*4.1.6.2. 2-((4-aminobutyl)amino)-3-(4-chlorophenyl)-7-methyl-5,6,7,8-tetrahydro pyrido[4′,3′:4,5]thieno[2,3-d]pyrimidin-4(3H)-one (**19**).* Using the general procedure above from compound **17** (0.102 g, 0.27 mmol) and butane-1,4-diamine (0.8 mL, 8.1 mmol) the title compound was obtained as a light-yellow sticky solid (0.062 g, 55%). $R_f = 0.20$ (DCM/MeOH, 8:2); IR: 3348, 2939, 1672, 1542 cm^{-1}; ^{1}HNMR (600 MHz, CD_3OD): δ 7.63 (d, $J = 8.7$ Hz, 2H), 7.32 (d, $J = 8.7$ Hz, 2H), 4.39 (bs, 2H), 3.55 (t, $J = 5.6$ Hz, 2H), 3.39 (t, $J = 6.1$ Hz, 2H), 3.23 (t, $J = 6.0$ Hz, 2H), 3.03 (s, 3H), 2.94 (t, $J = 7.1$ Hz, 2H), 1.67 – 1.61 (m, 4H); ^{13}C NMR (75 MHz, CD_3OD): δ 169.1, 160.1, 153.0, 136.7, 134.0, 131.6, 128.6, 118.1, 113.4, 52.5, 52.0, 43.0, 41.7, 40.2, 26.9, 25.5, 24.1; ESI-MS: *m/z* 418.2 $[M+H]^+$; ESI-HRMS: *m/z* $[M+H]^+$ calcd for $C_{20}H_{25}ON_5ClS$ $[M+H]^+$, 418.1463, found 418.1451.

*4.1.7. 3-(4-chlorophenyl)-2-((3-hydroxypropyl)amino)-7-methyl-5,6,7,8-tetrahydropyrido[4′,3′:4,5]thieno[2,3-d]pyrimidin-4(3H)-one (**20**)*

To a rb-flask compound **17** (0.102 g, 0.27 mmol) and 3-aminopropan-1-ol (1.0 mL, 13 mmol) were added and the reaction mixture was stirred for 16 h at 150 °C. Then, the mixture was allowed to cool down to rt and was partitioned between brine and DCM. The aqueous layer was further extracted twice with DCM and the combined organic layers were dried over Na_2SO_4 and evaporated to dryness. Compound **20** was obtained after FCC (DCM/MeOH 95:5) as a light-yellow sticky solid (0.050 g, 46%). $R_f = 0.35$ (DCM/MeOH, 9:1); IR: 3384, 2939, 1674, 1544 cm^{-1}; ^1H NMR (600 MHz, $CDCl_3$): δ 7.53 (d, $J = 8.0$ Hz, 2H), 7.22 (d, $J = 8.0$ Hz, 2H), 4.80 (t, $J = 5.4$ Hz, 1H), 3.62 (t, $J = 5.3$ Hz, 2H), 3.56 (bs, 2H), 3.54 – 3.51 (m, 2H), 3.45 (s, 1H), 3.00 (t, $J = 5.7$ Hz, 2H), 2.73 (t, $J = 5.7$ Hz, 2H), 2.48 (s, 3H), 1.69 (dt, $J = 11.1$ and 5.4 Hz, 2H); ^{13}C NMR (150 MHz, $CDCl_3$): δ 165.6, 158.6, 151.2, 136.1, 133.0, 131.0, 130.6, 129.3, 124.1, 114.3, 60.3, 53.6, 52.1, 45.5, 39.9, 31.8, 25.7; ESI-MS: *m/z* 405.2 $[M+H]^+$; ESI-HRMS: *m/z* $[M+H]^+$ calcd for $C_{19}H_{22}N_4O_2ClS$ $[M+H]^+$, 405.1147, found 405.1130.

*4.1.8. 3-(3-methoxyphenyl)-7-methyl-2-(methylthio)-5,6,7,8-tetrahydropyrido [4′,3′:4,5]thieno[2,3-d]pyrimidin-4(3H)-one (**21**)*

Compound **21** was synthesised according to the procedure described above for the preparation of compound **17**. Starting from **8** (0.2 g, 0.49 mmol) the title compound **21** was obtained as an orange solid (0.122 mg, 67%); $R_f = 0.49$ (DCM/MeOH, 9:1); ESI-MS: *m/z* 374.2 $[M+H]^+$, 388.2 $[M+Na]^+$; ^1H NMR (300 MHz, $CDCl_3$): δ 7.43 (t, $J = 8.1$ Hz, 1H), 7.05 (m, 1H), 6.88–6.85 (m, 1H), 6.82–6.80 (m, 1H), 3.84 (s, 3H), 3.65 (bs, 2H), 3.08 (t, $J = 5.7$ Hz, 2H), 2.76 (t, $J = 5.7$ Hz, 2H), 2.50 (s, 3H), 2.49 (s, 3H).

*4.1.9. General procedure for the synthesis of compounds **22**, **24** and **25***

To a rb-flask compound **21** (0.102 g, 0.27 mmol) and the appropriate amine were added and the reaction mixture was stirred for 72 h at the indicated temperature. Then, the mixture was left to cool down to rt and it was partitioned between brine and THF. The aqueous layer was further extracted twice with THF. The combined organic layers were dried over Na_2SO_4 and evaporated to dryness. The desired compounds were obtained in pure form after FCC purification (DCM/MeOH 2:8 to MeOH/25% NH_4OH 10:1).

*4.1.9.1. 2-((2-aminoethyl)amino)-3-(3-methoxyphenyl)-7-methyl-5,6,7,8-tetrahydropyrido[4′,3′:4,5]thieno[2,3-d]pyrimidin-4(3H)-one (**22**).* Using the general procedure above compound **21** (0.102 g, 0.27 mmol) and ethane-1,2-diamine (0.65 mL, 9.7 mmol) compound **22** along with by-product **23** were obtained.

*Compound **22**.* yellow sticky solid (0.022 g, 20%), $R_f = 0.56$ (MeOH/25% NH_4OH 99:1); IR: 3344, 3033, 1656, 1539 cm^{-1}; ^1H NMR (600 MHz, CD_3OD): δ 7.53 (t, $J = 8.1$ Hz, 1H), 7.14 (dd, $J = 8.3$ and 1.9 Hz, 1H), 6.94 (s, 1H), 6.91 (d, $J = 8.3$ Hz, 1H), 3.85 (s, 3H), 3.64–3.59 (m, 4H), 3.08 (t, $J = 5.8$ Hz, 2H), 2.99 (t, $J = 5.4$ Hz, 2H), 2.80 (t, $J = 5.8$ Hz, 2H), 2.50 (s, 3H);^{13}C NMR (75 MHz, CD_3OD): δ 167.7, 162.8, 160.5, 153.2, 136.6, 132.3, 129.9, 124.8, 121.9, 116.9, 115.7, 115.2, 56.1, 54.1, 52.9, 45.4, 41.1, 41.1, 26.7; ESI-MS: *m/z* 386.2 $[M+H]^+$; ESI-HRMS: *m/z* $[M+H]^+$ calcd for $C_{19}H_{24}O_2N_5S$ $[M+H]^+$ 386.1645, found 386.1638.

*4.1.9.2. 8-methyl-2,3,6,7,8,9-hexahydroimidazo[1,2-a]pyrido[4′,3′:4,5]thieno[2,3-d]pyrimidin-5(1H)-one (**23**).* Isolated as light yellow sticky solid (0.028 g, 40%), $R_f = 0.31$ (MeOH 100%); IR: 3147, 2927, 1664, 1610 cm^{-1}; ^1H NMR (600 MHz, CD_3OD): δ 4.17 (t, $J = 8.6$ Hz, 2H), 3.77 (t, $J = 8.6$ Hz, 2H), 3.54 (s, 2H), 3.02 (t, $J = 5.9$ Hz, 2H), 2.77 (t, $J = 5.9$

Hz, 2H), 2.45 (s, 3H); ^{13}C NMR (75 MHz, CD_3OD): δ 168.5, 159.5, 157.5, 129.5, 124.6, 54.1, 52.9, 45.4, 43.6, 41.6, 26.7; ESI-MS: *m/z* 263.1 $[M+H]^+$; ESI-HRMS: *m/z* $[M+H]^+$ calcd for $C_{12}H_{15}ON_4S$ $[M+H]^+$ 263.0957, found 263.0957.

*4.1.9.3. 2-((3-aminopropyl)amino)-3-(3-methoxyphenyl)-7-methyl-5,6,7,8-tetrahydropyrido[4′,3′:4,5]thieno[2,3-d]pyrimidin-4(3H)-one **(24)***. Using the general procedure above compound **21** (0.102 g, 0.27 mmol) and propane-1,3-diamine (0.82 mL, 9.8 mmol) compound **24** was obtained as a yellow sticky solid (0.011 g, 10%); R_f = 0.3 (MeOH/25% NH_4OH 95:5); IR: 3342, 2970, 1642, 1542 cm^{-1}; ^{1}H NMR (600 MHz, CD_3OD): δ 7.51 (t, *J* = 8.1 Hz, 1H), 7.12 (dd, *J* = 8.3, 1.9 Hz, 1H), 6.89 (t, *J* = 2.1 Hz, 1H), 6.86 (dd, *J* = 8.3 and 1.9, 1H), 3.85 (s, 3H), 3.60 (bs, 2H), 3.45–3.37 (m, 2H), 2.99 (t, *J* = 5.3 Hz, 2H), 2.79 (t, *J* = 5.7 Hz, 2H), 2.67 (t, *J* = 6.8 Hz, 2H), 2.48 (s, 3H), 1.76–1.67 (m, 2H);^{13}C NMR (75 MHz, CD_3OD): δ 168.3, 162.9, 160.7, 153.0, 136.9, 132.3, 129.8, 124.3, 121.9, 116.9, 115.6, 114.5, 56.1, 54.1, 52.9, 45.4, 40.1, 39.5, 32.4, 26.8; ESI-MS: *m/z* 400.2 $[M+H]^+$; ESI-HRMS: *m/z* $[M+H]^+$ calcd for $C_{20}H_{26}O_2N_5S$ $[M+H]^+$ 400.1802, found 400.1792.

*4.1.9.4. 3-(3-methoxyphenyl)-7-methyl-2-((2-(piperazin-1-yl)ethyl)amino)-5,6,7,8-tetrahydropyrido[4′,3′:4,5]thieno[2,3-d]pyrimidin-4(3H)-one **(25)***. Using the general procedure above compound **21** (0.102 g, 0.27 mmol) and 3-(piperazin-1-yl)propan-1-amine (2.0 mL, 15.2 mmol) compound **25** was obtained. as a yellow sticky solid (0.042 g, 34%); R_f = 0.56 (MeOH/25% NH_4OH 5:1.2); IR: 3326, 2941, 2833, 1672, 1544 cm^{-1}; ^{1}H NMR (600 MHz, CD_3OD): δ 7.53 (t, *J* = 8.1 Hz, 1H), 7.14 (dd, *J* = 8.4 and 2.3 Hz, 1H), 6.92 (t, *J* = 2.1 Hz, 1H), 6.89 (d, *J* = 8.4 Hz, 1H), 3.84 (s, 3H), 3.58 (s, 2H), 3.41 (t, *J* = 6.2 Hz, 2H), 2.97 (t, *J* = 5.7 Hz, 2H), 2.79–2.76 (m, 6H), 2.49 (t, *J* = 6.0 Hz, 2H), 2.48 (s, 3H), 2.43 (bs, 4H); ^{13}C NMR (75 MHz, CD_3OD):δ 168.1, 162.9, 160.5, 152.6, 137.0, 132.4, 129.9, 124.4, 122.0, 116.7, 115.8, 114.8, 57.0, 56.2, 54.1, 53.0, 52.9, 45.8, 45.4, 39.0, 26.8; ESI-MS: *m/z* 455.1 $[M+H]^+$; ESI-HRMS: *m/z* $[M+H]^+$ calcd for $C_{23}H_{31}O_2N_6S$ $[M+H]^+$ 455.2224, found 455.2211.

*4.1.10. Ethyl 2-amino-4,5,6,7-tetrahydrobenzo[b]thiophene-3-carboxylate **(27)***

Compound **27** was synthesised according to the method for the synthesis of compound **3**, using cyclohexanone **26** (2.59 g, 25.0 mmol), sulfur (0.8 g, 25.0 mmol), ethyl cyanoacetate **2** (2.66 mL, 25.0 mmol). The title compound **27** was obtained as a yellow solid (2.89 g, 52%) following recrystallisation from methanol; R_f = 0.37 (petroleum ether/EtOAc 9:1); m.p 102–106 °C (lit.[36] – 107 °C); ^{1}H NMR (600 MHz, $CDCl_3$):δ 4.24 (q, *J* = 7.1 Hz, 2H), 2.68 (t, *J* = 5.3 Hz, 2H), 2.47 (t, *J* = 5.3 Hz, 2H), 1.79–1.69 (m, 4H), 1.32 (t, *J* = 7.1 Hz, 3H); ^{13}C NMR (75 MHz, $CDCl_3$):δ 166.1, 161.6, 132.5, 117.7, 105.8, 59.4, 26.9, 24.5, 23.2, 22.8, 14.5; ESI-MS: *m/z* 226.0 $[M+H]^+$.

*4.1.11. Ethyl 2-(3-(3-methoxyphenyl)thioureido)-4,5,6,7-tetrahydrobenzo[b]thiophene-3-carboxylate **(28)***

To a solution of **27** (0.1 g, 0.44 mmol) in anhydrous pyridine (1 mL), 3-methoxyphenyl isothiocyanate (**5**) (0.08 mL, 0.58 mmol) was added dropwise. The reaction mixture was stirred at 45 °C for 16 h. Pyridine was evaporated, and the residue was subjected to FCC (Petroleum ether/EtOAc 95:5 to 85:15) to give the title compound as a light-yellow solid (0.165 g, 95%). R_f = 0.56 (Petroleum ether/EtOAc 8:2); ^{1}HNMR (600 MHz, $CDCl_3$): δ 12.21 (s, 1H), 8.13 (s, 1H), 7.32 (t, *J* = 8.3 Hz, 1H), 6.88–6.85 (m, 3H), 4.12 (q, *J* = 7.1 Hz, 2H), 3.80 (s, 3H), 2.70 (t, *J* = 5.8 Hz, 2H), 2.61 (t, *J* = 5.7 Hz, 2H), 1.77–1.72 (m, 4H), 1.23 (t, *J* = 7.1 Hz, 3H); ^{13}CNMR (75 MHz, $CDCl_3$): δ 175.8, 166.3, 160.7, 149.8, 136.9, 130.8, 130.6, 126.9, 117.2, 113.8, 113.1, 110.5, 60.4, 55.4, 26.3, 24.3, 23.0, 22.8, 14.2; ESI-MS: *m/z* 391.0 $[M+H]^+$.

*4.1.12. 3-(3-methoxyphenyl)-2-(methylthio)-5,6,7,8-tetrahydrobenzo[4,5]thieno[2,3-d]pyrimidin-4(3H)-one **(30)***

Compound **30** was synthesised according to the method described above for the preparation of compound **17**, using compound **28** (0.16 g, 0.42 mmol) and iodomethane (0.26 mL, 0.42 mmol), as a white solid which was used to the next step without further purification. R_f = 0.26 (Petroleum ether/EtOAc, 9:1); ESI-MS: *m/z* 359.2$[M+H]^+$.

*4.1.13. 2-((2-aminoethyl)amino)-3-(3-methoxyphenyl)-5,6,7,8-tetrahydrobenzo[4,5]thieno[2,3-d]pyrimidin-4(3H)-one **(31)***

Compound **31** was synthesized according to the method described above for the synthesis of **22** from compound **30** (0.150 g, 0.42 mmol) and 1,2-diamino ethane (2.0 mL, 29 mmol) after FCC purification (EtOAc/MeOH 9:1), as a light-yellow oil (0.096 g, 62%); R_f = 0.12 (EtOAc/MeOH 9:1). Compound **31** was then dissolved in MeOH (0.5 mL), and an equimolar amount of oxalic acid was added and the corresponding salt was precipitated as a white solid by the addition of diethyl ether, filtered and dried (0.107 g, 90%); m.p: 148–151 °C; IR: 3352, 2937, 1737, 1654, 1542 cm^{-1}; ^{1}H NMR (600 MHz, CD_3OD): δ 7.46 (t, *J* = 8.1 Hz, 1H), 7.03 (d, *J* = 8.1 Hz, 1H), 6.87 (d, *J* = 8.1 Hz, 1H), 6.81 (s, 1H), 4.76 (t, *J* = 5.1 Hz, 1H), 3.82 (s, 3H), 3.48–3.40 (m, 2H), 2.90–2.83 (m, 4H), 2.68 (t, *J* = 5.2 Hz, 2H), 1.88–1.75 (m, 4H); ^{13}C NMR (75 MHz, CD_3OD): δ 165.2, 161.4, 158.9, 150.8, 135.9, 131.42, 131.38, 127.2, 120.9, 115.9, 115.0, 114.5, 55.7, 43.5, 40.7, 25.6, 25.1, 23.4, 22.6; ESI-MS: *m/z* 371.2 $[M+H]^+$; ESI-HRMS: *m/z* $[M+H]^+$ calcd for $C_{19}H_{23}O_2N_4S$ $[M+H]^+$ 371.1536, found 371.1528.

*4.1.14. 2-((3-aminopropyl)amino)-3-(3-methoxyphenyl)-5,6,7,8-tetrahydrobenzo[4,5]thieno[2,3-d]pyrimidin-4(3H)-one **(32)***

Compound **32** was synthesized according to the method described above for the synthesis of **22**, from compound **30** (0.184 g, 0.51 mmol) and 1,3-diaminopropane (2 mL, 23.9 mmol) after FCC purification (EtOAc/MeOH 9:1), as a light-yellow oil (0.147 g, 74%); R_f = 0.12 (DCM/MeOH 8:2). Compound **32** was then dissolved in MeOH (0.5 mL) and an equimolar amount of oxalic acid was added and the corresponding salt was precipitated as a white solid by the addition of diethyl ether, filtered and dried (0.198 g, 92%); m.p: 79–82 °C; IR: 3359, 2929, 1740, 1654, 1542 cm^{-1}; ^{1}H NMR (600 MHz, CD_3OD): δ 7.52 (t, *J* = 8.1 Hz, 1H), 7.13 (dd, *J* = 8.5 and 2.5 Hz, 1H), 6.91 (t, *J* = 2.4 Hz, 1H), 6.87 (dd, *J* = 8.5 and 2.5, 1H), 3.84 (s, 3H), 3.44 (dd, *J* = 14.5 and 6.6 Hz, 2H), 2.93 (t, *J* = 7.3 Hz, 2H), 2.81 (t, *J* = 6.0 Hz, 2H), 2.68 (t, *J* = 6.0 Hz, 2H), 1.91–1.85 (m, 4H), 1.81–1.78 (m, 2H);^{13}C NMR (150 MHz, CD_3OD):δ 167.0, 162.8, 160.6, 152.7, 136.9, 132.4, 131.9, 128.3, 121.9, 116.8, 115.7, 115.5, 56.1, 39.3, 38.4, 29.0, 26.6, 25.7, 24.3, 23.5; ESI-MS: *m/z* 385.1 $[M+H]^+$; ESI-HRMS: *m/z* $[M+H]^+$ calcd for $C_{20}H_{25}O_2N_4S$ $[M+H]^+$, 385.1693, found 385.1682.

*4.1.15. 3-(3-methoxyphenyl)-2-((2-(piperazin-1-yl)ethyl)amino)-5,6,7,8 tetrahydrobenzo[4,5]thieno[2,3-d]pyrimidin-4(3H)-one **(33)***

Compound **33** was synthesized according to the method described above for the synthesis of **22** from compound **30** (0.106 g, 0.29 mmol) and 1-(2-aminoethyl)piperazine (2 mL, 15.2 mmol) after FCC purification (MeOH/25% NH_4OH 9:1) as a light-yellow sticky solid (0.024 g, 20%); R_f = 0.37 (DCM/MeOH/8:2); IR: 3336, 2941, 1676, 1546 cm^{-1}; ^{1}H NMR (600 MHz, CD_3OD): δ 7.54 (t, *J* = 8.1 Hz, 1H), 7.15 (dd, *J* = 8.5 and 1.7 Hz, 1H), 6.92 (t, *J* = 1.8 Hz, 1H), 6.89 (dd, *J* = 8.5 and 1.7 Hz, 1H), 3.85 (s, 3H), 3.40 (t, *J* = 6.2 Hz, 2H), 2.82 (t, *J* = 6.0 Hz, 2H), 2.68 (bs, 6H), 2.46 (t, *J* = 6.2 Hz, 2H), 2.36 (bs, 4H), 1.90–1.85 (m, 2H), 1.81–1.77 (m, 2H); ^{13}C NMR (75 MHz, CD_3OD):δ 167.5, 162.9, 160.6, 152.3, 137.2, 132.4, 131.8, 128.1, 122.0, 116.6, 115.8, 115.3, 57.2, 56.2, 53.9, 46.1, 39.0, 26.7, 25.7, 24.3, 23.6; ESI-MS: *m/z* 440.2 $[M+H]^+$; ESI-HRMS: *m/z* $[M+H]^+$ calcd for $C_{23}H_{30}O_2N_5S$ $[M+H]^+$, 440.2115, found 440.2104.

4.2. In vitro evaluation of antimicrobial and antifungal activity

Microbial culture treated isolates: The antibacterial and antifungal activity of all investigated samples was tested on strains obtained from the Mycological laboratory, Department of Plant Physiology, Institute for Biological Research "Siniša Stanković" National Institute of Republic of Serbia, Belgrade, Serbia. The following Gram (+) bacteria (*Bacillus cereus* clinical isolate, *Micrococcus flavus* ATCC 10240, *Staphylococcus aureus* ATCC 6538 and *Listeria monocytogenes* NCTC 7973), Gram (-) bacteria (*Escherichia coli* ATCC 35210, *Enterobacter cloacae* human isolate, *Pseudomonas aeruginosa* ATCC 27853 and *Salmonella Typhimurium* ATCC 13311) and micromycetes *Aspergillus fumigatus* (ATCC 1022), *Aspergillus versicolor* (ATCC 11730), *Aspergillus ochraceus* (ATCC 12066), *Aspergillus niger* (ATCC 6275), *Trichoderma viride* (IAM 5061), *Penicillium funiculosum* (ATCC 36839), *Penicillium ochrochloron* (ATCC 9112) and *P. verrucosum* var. *cyclopium* (food isolates) were tested. Bacterial strains were grown in Tryptic Soy Broth (TSB) at 37 °C for 24 h. After harvesting, microbial cells were suspended in sterile saline solution a concentration of approximately 1.0×10^6 CFU ml^{-1} and immediately used. Fungi were maintained in solid Malt Agar (MA) medium at 120 h at 28 °C. The fungal spores were washed from the surface of agar plates with sterile 0.85% saline containing 0.1% Tween 80 (v/v). The spore suspension was adjusted with sterile saline to a concentration of approximately 1.0×10^5 in a final volume of 100 μL per well. The cultures were subcultured once a month and stored at +4 °C for further usage [37].

Micro-well dilution assay: For the determination of the antimicrobial activity of tested compounds, a modified microdilution method was used [38–40]. The assay was performed by using sterile 96-well microtiter plates. Compounds were dissolved in 5% DMSO (1 mg/ml) and the corresponding media – TSB and MB for bacteria and fungi, respectively. The microplates were incubated for 24 h at 37 °C for bacterial and for 72 h at 28 °C for fungal strains, respectively. The results were presented as minimum inhibitory concentrations (MIC), minimum bactericidal concentrations (MBC) and minimum fungicidal concentrations (MFC). DMSO was used as a negative control, and commercial antibiotics streptomycin and ampicillin, and commercial fungicides, bifonazole and ketoconazole, were used as positive controls. All experiments were performed in duplicate and repeated three times.

4.3. Cell culture and cell viability assay

HFL-1 human embryonic primary fibroblasts were obtained from the European Collection of Cell Cultures and were maintained in a humidified incubator (37 °C and 5% CO_2, 95% humidity) in Dulbecco's Modified Eagle's Medium (DMEM; Invitrogen, Carlsbad, CA, USA) supplemented with 10% fetal bovine serum (Invitrogen, Carlsbad, CA, USA), 2 mM glutamine, 1% non-essential amino acids and 1% penicillin–streptomycin (complete medium). Early passage cells (CPD < 37) were maintained for 24 and 48 h in complete medium containing 0.027 and 0.058 mM compound **15** and 0.05 and 0.26 mM compound **22** or dimethyl sulfoxide (DMSO; control). The percentage of cell survival was determined through crystal violet staining. HFL-1 cells treated as described above were fixed in 4% paraformaldehyde for 20 min at 37 °C and then stained with 0.2% crystal violet in distilled water. The cells were then washed with ddH_2O and the dye was eluted with 30% acetic acid. Viability was monitored via measurement of the dye absorbance at 595 nm using the Safire2 Multi-detection Microplate Reader (Tecan, Grödig, Austria). Each sample was seeded in five replicates in 3 independent experiments.

4.4. Evaluation of in vivo toxicity

4.4.1. Strains and nematode cultures

We followed standard procedures for strain maintenance at 20 °C. *C. elegans* strain N2 (wild type Bristol isolate; wt) was used during the course of the experiment, provided by the CGC, which is funded by NIH Office of Research Infrastructure Programs (P40 OD010440).

4.4.2. Compound treatment

Nematodes were exposed to the following final designated concentrations per NGM plate: 0.027 and 0.058 mM compound **15** and 0.05 and 0.26 mM compound **22**, corresponding to MIC/MFC (for compound **15**) and MIC/MBC (for compound **22**), respectively. Stock solutions of the tested compounds were prepared after suspension in DMSO and were kept at −20 °C. The appropriate amount of the tested compounds or DMSO (<1%) (control cultures) [41] were added on UV-irradiated OP50 bacteria lawn. UV-killed bacteria were used to avoid the side effects of living bacteria metabolism.

4.4.3. Toxicity test in the nematode Caenorhabditis elegans though phenotypic analysis

For all assays, N2 adult nematodes were set to lay eggs for 30 min on NGM plates containing the tested compounds or the appropriate amount of DMSO (control cultures). For the pharyngeal pumping and defecation assays the nematodes were transferred to plates containing the tested compounds or DMSO at the L4 stage. Standard procedures were followed as described before [42]. More specifically:

4.4.3.1. Developmental timing. The progeny were frequently observed to record the necessary time to reach the L4 larval stage from egg hatching. The experiment was repeated five times.

4.4.3.2. Pharyngeal pumping. At days 1 and 3 of adulthood, the pharyngeal pumping rate was assessed for 15 s and expressed as number of pumps/min. At least 30 animals per condition were evaluated.

4.4.3.3. Defecation assay. At days 1 and 3 of adulthood, the period in seconds needed from defecation to defecation (defecation rate) was recorded. At least 30 animals per condition were evaluated.

4.4.4. Statistical analysis

One-way ANOVA followed by Tukey's and Dunnett's tests were applied to compare the means between the groups. The statistical significance level was set at $p < 0.05$. The results are expressed as means ± standard error of the means (SEM) of three independent experiments. Asterisks denote p-values as follows: $^*p < 0.05$, $^{**}p < 0.01$, $^{***}p < 0.001$. Statistical analyses were performed using the SPSS software (version 20.0; IBM Corp., Armonk, NY, USA).

4.5. Similarity search and molecular docking studies

Structural similarity search was applied using the online platform ChemMine Tools (http://chemmine.ucr.edu) [43]. Compounds **22** and **15**, presenting the higher antibacterial and antifungal activity respectively, were imported as the reference molecules for similarity search. PubChem fingerprint algorithm was selected with a similarity cutoff equal to 0.5.

S. aureus topoisomerase II DNA gyrase, co-crystallized with ciprofloxacin and DNA (PDB:2XCT) was selected for molecular docking of compounds **14** and **22** while a homology model of *A. fumigatus* CYP51A was used for docking compounds **14** and **15**.

Molecular simulations were performed using Schrödinger Suite Release 2020–3. In an initial step, the examined targets and compounds were prepared using the Protein Preparation Wizard [44] and LigPrep [45], respectively. Molecular docking simulations were performed, applying the Extra Precision (XP) mode and Standard Presision (SP) mode of Glide and a grid box with dimensions 10 × 10 × 10 Å was generated for both enzymes [46]. The number of poses were set equal to 10 and were visually inspected [47].

For validation of docking parameters, the co-crystallized ligand

ciprofloxacin and econazole were re-docked into the active site of topoisomerase II gyrase and CYP51A, respectively. The results indicate an almost identical binding pattern (Fig. S1, Supplementary Material).

4.6. Calculation of molecular descriptors

QikProp (Schrödinger Suite Release 2020–3) was utilized to generate molecular descriptors and properties (Table S3 Supplementary Material for the synthesized compounds.

4.7. Pharma RQSAR models

Scaffold decomposition and R-group analysis panels of Canvas [48] have been combined to identify the core scaffold (Fig. 4B) and the types of chemical groups that are most important for the antimicrobial and antifungal activity of the examined compounds at each attachment point. For this scope, the experimental MIC values (mM) of the examined compounds were converted to appropriate form for QSAR studies (log (1/MIC) values). For the Pharma RQSAR models construction, a partial-least-squares (PLS) process was utilized to fit the examined compounds. Randomly, the module assigns the 75% and the 25% of compounds as training and test set, respectively. The procedure was repeated many times and the mean of coefficients from the best models were determined, offering information about the significance of the log(1/MIC).

Representation of the Pharma RQSAR models and the minimum, maximum, mean and standard deviation values for the PLS coefficient are presented in Supplementary Material (Tables S1, S2 and Figs. S2, S3).

Declaration of Competing Interest

The authors declare that they have no known competing financial interests or personal relationships that could have appeared to influence the work reported in this paper.

Acknowledgments

We acknowledge support of this work by the project “OPENSCREEN-GR: An Open-Access Research Infrastructure of Chemical Biology and Target-Based Screening Technologies for Human and Animal Health Agriculture and the Environment” “(2018–2020)” (MIS) 5002691 which is implemented under the Action “Reinforcement of the Research and Innovation Infrastructure”, funded by the Operational Programme “Competitiveness, Entrepreneurship and Innovation” (NSRF 2014-2020) and co-financed by Greece and the European Union (European Regional Development Fund).

This work has been supported by Ministry of Education, Science and Technological Development of Republic of Serbia (451-03-68/2020-14/200007).

Appendix A. Supplementary material

Supplementary data to this article can be found online at https://doi.org/10.1016/j.bioorg.2020.104509.

References

[1] WHO, Antimicrobial Resistance. IACG final report, April 2019.
[2] A.P. Taylor, R.P. Robinson, Y.M. Fobian, D.C. Blakemore, L.H. Jones, O. Fadeyi, Modern advances in heterocyclic chemistry in drug discovery, Org. Biomol. Chem. 14 (2016) 6611–6637, https://doi.org/10.1039/C6OB00936K.
[3] N.A. Meanwell, Chapter five - a synopsis of the properties and applications of heteroaromatic rings in medicinal chemistry, Adv. Heterocycl. Chem. 123 (2017) 245–361, https://doi.org/10.1016/bs.aihch.2016.11.002.
[4] M. Zhang, J. Tamiya, L. Nguyen, M.W. Rowbottom, B. Dyck, T.D. Vickers, J. Grey, D.A. Schwarz, C.E. Heise, J. Haelewyn, M.S. Mistry, V.S. Goodfellow, Thienopyrimidinone bis-aminopyrrolidine ureas as potent melanin-concentrating hormone receptor-1 (MCH-R1) antagonists, Bioorg. Med. Chem. Lett. 17 (2007) 2535–2539, https://doi.org/10.1016/j.bmcl.2007.02.012.
[5] Y. Kim, J. Kim, S. Kim, Y. Ki, S.H. Seo, J. Tae, M.K. Ko, H.S. Jang, E.J. Lim, C. Song, Y. Cho, H.Y. Koh, Y. Chong, I.H. Choo, G. Keum, S.J. Min, H. Choo, Novel thienopyrimidinones as mGluR1 antagonists, Eur. J. Med. Chem. 85 (2014) 629–637, https://doi.org/10.1016/j.ejmech.2014.08.027.
[6] A.R. Ekkati, V. Madiyan, K.P. Ravindranathan, J.H. Bae, J. Schlessinger, W. L. Jorgensen, Aryl extensions of thienopyrimidinones as fibroblast growth factor receptor 1 kinase inhibitors, Tetrahedron Lett. 52 (2011) 2228–2231, https://doi.org/10.1016/j.tetlet.2010.12.081.
[7] K. Hannigan, S.S. Kulkarni, V.G. Bdzhola, A.G. Golub, S.M. Yarmoluk, T.T. Talele, Identification of novel PARP-1 inhibitors by structure-based virtual screening, Bioorg. Med. Chem. Lett. 23 (2013) 5790–5794, https://doi.org/10.1016/j.bmcl.2013.09.007.
[8] S. Sundriyal, S. Moniot, Z. Mahmud, S. Yao, P. Di Fruscia, C.R. Reynolds, D. T. Dexter, M.J. Sternberg, E.W. Lam, C. Steegborn, M.J. Fuchter, Thienopyrimidinone based sirtuin-2 (SIRT2)-selective inhibitors bind in the ligand induced selectivity pocket, J. Med. Chem. 60 (2017) 1928–1945, https://doi.org/10.1021/acs.jmedchem.6b01690.
[9] K. Kawai, Y. Endo, T. Asano, S. Amano, K. Sawada, N. Ueo, N. Takahashi, Y. Sonoda, M. Nagai, N. Kamei, N. Nagata, Discovery of 2-(cyclopentylamino) thieno[3,2-d]pyrimidin-4(3H)-one derivatives as a new series of potent phosphodiesterase 7 inhibitors, J. Med. Chem. 57 (2014) 9844–9854, https://doi.org/10.1021/jm5008215.
[10] A. Cohen, P. Suzanne, J.C. Lancelot, P. Verhaeghe, A. Lesnard, L. Basmaciyan, S. Hutter, M. Laget, A. Dumètre, L. Paloque, E. Deharo, M.D. Crozet, P. Rathelot, P. Dallemagne, A. Lorthiois, C.H. Sibley, P. Vanelle, A. Valentin, D. Mazier, S. Rault, N. Azas, Discovery of new thienopyrimidinone derivatives displaying antimalarial properties toward both erythrocytic and hepatic stages of Plasmodium, Eur. J. Med. Chem. 95 (2015) 16–28, https://doi.org/10.1016/j.ejmech.2015.03.011.
[11] M.M. Pisal, L.U. Nawale, M.D. Patil, S.G. Bhansali, J.M. Gajbhiye, D. Sarkar, S. P. Chavan, H.B. Borate, Hybrids of thienopyrimidinones and thiouracils as anti-tubercular agents: SAR and docking studies, Eur. J. Med. Chem. 127 (2017) 459–469, https://doi.org/10.1016/j.ejmech.2017.01.009.
[12] T. Masaoka, S. Chung, P. Caboni, J.W. Rausch, J.A. Wilson, H. Taskent-Sezgin, J. A. Beutler, G. Tocco, S.F. Le Grice, Exploiting drug-resistant enzymes as tools to identify thienopyrimidinone inhibitors of human immunodeficiency virus reverse transcriptase-associated ribonuclease H, J. Med. Chem. 56 (2013) 5436–5445, https://doi.org/10.1021/jm400405z.
[13] A.A. Bekhit, A.M. Farghaly, R.M. Shafik, M.M.A. Elsemary, A.E.A. Bekhit, A. A. Guemei, M.S. El-Shoukrofy, T.M. Ibrahim, Synthesis, biological evaluation and molecular modeling of novel thienopyrimidinone and triazolothienopyrimidinone derivatives as dual anti-inflammatory antimicrobial agents, Bioorg. Chem. 77 (2018) 38–46, https://doi.org/10.1016/j.bioorg.2017.12.028.
[14] W. Zhong, K.K. Pasunooti, S. Balamkundu, Y.H. Wong, Q. Nah, V. Gadi, S. Gnanakalai, Y.H. Chionh, M.E. McBee, P. Gopal, S.H. Lim, N. Olivier, E. T. Buurman, T. Dick, C.F. Liu, J. Lescar, P.C. Dedon, Thienopyrimidinone derivatives that inhibit bacterial tRNA (Guanine37-N1)-methyltransferase (TrmD) by restructuring the active site with a tyrosine-flipping mechanism, J. Med. Chem. 62 (2019) 7788–7805, https://doi.org/10.1021/acs.jmedchem.9b00582.
[15] Puterová Z., Krutošíková A., Végh D., Gewald reaction: synthesis, properties and applications of substituted 2-aminothiophenes. ARKIVOC - Special Issue Reviews and Accounts ARKAT USA, Inc. (2010) 209–246. https://doi.org/10.3998/ark.5550190.0011.105.
[16] Blaskiewicz P., Vorbrueggen H., Koch H., Thieno (2,3-d) pyrimidinone derivs - for use as anti-inflammatories and inters, for antimicrobials, DE2411273 (A1), 1975.
[17] K. Wang, J. Li, A. Degterev, E. Hsu, J. Yuan, C. Yuan, Structure–activity relationship analysis of a novel necroptosis inhibitor, Necrostatin-5, Bioorg. Med. Chem. Lett. 17 (2007) 1455–1465, https://doi.org/10.1016/j.bmcl.2006.11.056.
[18] P.R. Hunt, The C. elegans model in toxicity testing, J. Appl. Toxicol. 37 (2017) 50–59, https://doi.org/10.1002/jat.3357.
[19] M.C.K. Leung, P.L. Williams, A. Benedetto, C. Au, K.J. Helmcke, M. Aschner, J. N. Meyer, Caenorhabditis elegans: an emerging model in biomedical and environmental toxicology, Toxicol. Sci. 106 (2008) 5–28, https://doi.org/10.1093/toxsci/kfn121.
[20] ASTM Int. (2014).
[21] R. Dhawan, D.B. Dusenbery, P.L. Williams, A comparison of metal-induced lethality and behavioral responses in the nematode Caenorhabditis elegans, Environ. Toxicol. Chem. 19 (2000) 3061–3067, https://doi.org/10.1002/etc.5620191228.
[22] G.L. Anderson, W.A. Boyd, P.L. Williams, Assessment of sublethal endpoints for toxicity testing with the nematode Caenorhabditis elegans, Environ. Toxicol. Chem. 20 (2001) 833–838, https://doi.org/10.1002/etc.5620200419.
[23] L. Aitlhadj, S.R. Stürzenbaum, The toxicological assessment of two anti-obesity drugs in C. elegans, Toxicol. Res. (Camb). 2 (2013) 145–150, https://doi.org/10.1039/c2tx20096a.
[24] T. Lieke, X. Zhang, C.E.W. Steinberg, B. Pan, Overlooked risks of biochars: persistent free radicals trigger neurotoxicity in Caenorhabditis elegans, Environ. Sci. Technol. 52 (2018) 7981–7987, https://doi.org/10.1021/acs.est.8b01338.
[25] D. Baderna, A. Colombo, M. Romeo, F. Cambria, F. Teoldi, M. Lodi, L. Diomede, E. Benfenati, Soil quality in the Lomellina area using in vitro models and ecotoxicological assays, Environ. Res. 133 (2014) 220–231, https://doi.org/10.1016/j.envres.2014.05.030.

[26] J. Choi, Caenorhabditis elegans as a biological model for multilevel biomarker analysis in environmental toxicology and risk assessment, Toxicol. Res. 24 (2008) 235–243, https://doi.org/10.5487/TR.2008.24.4.235.
[27] P.R. Hunt, N. Olejnik, K.D. Bailey, C.A. Vaught, R.L. Sprando, C. elegans development and activity test detects mammalian developmental neurotoxins, Food Chem. Toxicol. 121 (2018) 583–592, https://doi.org/10.1016/j.fct.2018.09.061.
[28] M.A. Johnson, G.M. Maggiora. Concepts and Applications of Molecular Similarity, Wiley, 1990, https://doi.org/10.1002/jcc.540130415.
[29] N.A. Kahlous, M.A.M. Bawarish, M.A. Sarhan, M. Küpper, A. Hasaba, M. Rajab, Using chemoinformatics, bioinformatics, and bioassay to predict and explain the antibacterial activity of nonantibiotic food and drug administration drugs, ASSAY Drug Dev. Techn. 15 (2017) 89–105, https://doi.org/10.1089/adt.2016.771.
[30] K.F. Croom, K.L. Goa, Levofloxacin: a review of its use in the treatment of bacterial infections in the United States, Drugs 63 (2003) 2769–2802, https://doi.org/10.2165/00003495-200363240-00008.
[31] B.D. Bax, P.F. Chan, D.S. Eggleston, A. Fosberry, D.R. Gentry, F. Gorrec, I. Giordano, M.M. Hann, A. Hennessy, M. Hibbs, J. Huang, E. Jones, J. Jones, K. K. Brown, C.J. Lewis, E.W. May, M.R. Saunders, O. Singh, C.E. Spitzfaden, C. Shen, A. Shillings, A.J. Theobald, A. Wohlkonig, N.D. Pearson, M.N. Gwynn, Type IIA topoisomerase inhibition by a new class of antibacterial agents, Nature 466 (2010) 935–940, https://doi.org/10.1038/nature09197.
[32] S. Campoy, J.L. Adrio, Antifungals, Biochem. Pharmacol. 133 (2017) 86–96, https://doi.org/10.1016/j.bcp.2016.11.019.
[33] E. Kritsi, M.T. Matsoukas, C. Potamitis, A. Detsi, M. Ivanov, M. Sokovic, P. Zoumpoulakis, Novel hit compounds as putative antifungals: the case of *Aspergillus fumigatus*, Molecules 24 (2019) 3853, https://doi.org/10.3390/molecules24213853.
[34] Patel M.M., Patel L.J., Design, Synthesis, molecular docking, and antibacterial evaluation of some novel flouroquinolone derivatives as potent antibacterial agent, Sci. World J. (2014), Article ID 897187, https://doi.org/10.1155/2014/897187.
[35] F.E.M. El-Baih, H.A.S. Al-Blowy, H.M. Al-Hazimi, Synthesis of some thienopyrimidine derivatives, Molecules 11 (2006) 498–513, https://doi.org/10.3390/11070498.
[36] A. Flood, C. Trujillo, G. Sanchez-Sanz, B. Kelly, C. Muguruza, L.F. Callado, I. Rozas, Thiophene/thiazole-benzene replacement on guanidine derivatives targeting α2-Adrenoceptors, Eur. J. Med. Chem. 138 (2017) 38–50, https://doi.org/10.1016/j.ejmech.2017.06.008.
[37] J. Glamočlija, A. Ćirić, M. Nikolić, Â. Fernandes, L. Barros, R.C. Calhelha, I.C.F. R. Ferreira, M. Soković, L.J.L.D. van Griensven, Chemical characterization and biological activity of Chaga (Inonotus obliquus), a medicinal "mushroom", J. Ethnopharmacol. 162 (2015) 323–332, https://doi.org/10.1016/j.jep.2014.12.069.
[38] Clinical and Laboratory Standards Institute, Methods for Dilution Antimicrobial Susceptibility Test For Bacteria That Grow Aerobically in: Approved Standards. 8th ed. CLSI Publication, Wayne, PA, M07-A8, 2009.
[39] H. Hänel, W. Raether, A more sophisticated method of determining the fugicidal effect of water-insoluble preparations with a cell harvester, using miconazole as an example, Mycoses 31 (1988) 148–154, https://doi.org/10.1111/j.1439-0507.1988.tb03718.x.
[40] T. Tsukatani, H. Suenaga, M. Shiga, K. Noguchi, M. Ishiyama, T. Ezoe, K. Matsumoto, Comparison of the WST-8 colorimetric method and the CLSI broth microdilution method for susceptibility testing against drug-resistant bacteria, J. Microbiol. Methods 90 (2012) 160–166, https://doi.org/10.1016/j.mimet.2012.05.001.
[41] H. Frankowski, S. Alavez, P. Spilman, K.A. Mark, J.D. Nelson, P. Mollahan, R. V. Rao, S.F. Chen, G.J. Lithgow, H.M. Ellerby, Dimethyl sulfoxide and dimethyl formamide increase lifespan of C. elegans in liquid, Mech. Ageing Dev. 134 (2013) 69–78, https://doi.org/10.1016/j.mad.2012.10.002.
[42] N. Papaevgeniou, A. Hoehn, J.A. Tur, L.O. Klotz, T. Grune, N. Chondrogianni, Sugar-derived AGEs accelerate pharyngeal pumping rate and increase the lifespan of Caenorhabditis elegans, Free Radic. Res. 53 (sup1) (2019) 1056–1067, https://doi.org/10.1080/10715762.2019.1661403.
[43] T.W.H. Backman, Y. Cao, T. Girke, ChemMine tools: an online service for analyzing and clustering small molecules, Nucleic Acids Res. 39 (2011) 486–491, https://doi.org/10.1093/nar/gkr320.
[44] Protein Preparation Wizard; Epik, Schrödinger, LLC, New York, NY, 2016; Impact, Schrödinger, LLC, New York, NY, 2016; Prime, Schrödinger, LLC, New York, NY, 2020.
[45] Schrödinger Release 2020-3: LigPrep, Schrödinger, LLC, New York, NY, 2020.
[46] Schrödinger Release 2020-3: Glide, Schrödinger, LLC, New York, NY, 2020.
[47] Schrödinger Release 2020-3: Maestro, Schrödinger, LLC, New York, NY, 2020.
[48] Canvas, Schrödinger, LLC, New York, NY, 2019.